Communications Earth & Environment https://doi.org/10.1038/s43247-026-03633-6

Article in Press

Human ignitions dominate the fire regimes of the Brazilian Cerrado

Received: 15 July 2025

Accepted: 6 May 2026

Cite this article as: Segura-Garcia, C., Janssen, T.A., Libonati, R. *et al.* Human ignitions dominate the fire regimes of the Brazilian Cerrado. *Commun Earth Environ* (2026). https://doi.org/10.1038/s43247-026-03633-6

Carlota Segura-Garcia, Thomas A. J. Janssen, Renata Libonati, Lucas S. Menezes, Guilherme Mataveli, Sander Veraverbeke, Matthew W. Jones & Imma Oliveras Menor

Human ignitions dominate the fire regimes of the Brazilian Cerrado

Carlota Segura-Garcia[1,*], Thomas A. J. Janssen[2], Renata Libonati[3,4], Lucas S. Menezes[3], Guilherme Mataveli[5,6], Sander Veraverbeke[6,7], Matthew W. Jones[6], and Imma Oliveras Menor[1,8]

[1]Environmental Change Institute, School of Geography and the Environment, University of Oxford, Oxford, UK

[2]Plant Ecology and Nature Conservation, Department of Environmental Sciences, Wageningen University, Wageningen, The Netherlands

[3]Departamento de Meteorologia, Universidade Federal do Rio de Janeiro, Rio de Janeiro, Brazil

[4]Universidade de Lisboa, Faculdade de Ciências, Instituto Dom Luiz, Lisboa, Portugal

[5]Earth Observation and Geoinformatics Division and Tropical Ecosystems and Environmental Sciences Laboratory, National Institute for Space Research (INPE), São José dos Campos, São Paulo, Brazil

[6]Tyndall Centre for Climate Change Research, School of Environmental Sciences, University of East Anglia, Norwich Research Park, Norwich, UK

[7]Faculty of Science, Vrije Universiteit Amsterdam, Amsterdam, The Netherlands

[8]AMAP, Univ Montpellier, CIRAD, CNRS, INRAE, IRD, Montpellier, France

[*]Corresponding author: carlotasegurag@gmail.com

May 1, 2026

Abstract

Before human settlement, lightning was the predominant ignition source shaping the expansion of fire-adapted savannas and grasslands such as the Cerrado. However, humans have since altered ignition frequency, timing and intensity of fires, further influencing

these ecosystems. Even though humans are considered the main cause of fires in the tropics, no study has quantitatively disentangled the relative contributions of lightning and human ignitions across the entire Cerrado. Here, we present a region-wide assessment of lightning and human-caused fire regimes, linking individual fire events and lightning occurrence through an attribution algorithm. We show that humans account for nearly 90% of ignitions, effectively redefining the natural fire regime of the Cerrado. Lightning ignitions peak during the dry-to-wet transition, whereas humans ignite fires throughout the dry season extending its duration threefold. Further, humans disproportionately drive fires with extreme behaviour, which have outsized ecological impacts, by igniting fires about ten times larger or two times more intense than lightning. These findings highlight the dominant role of humans in shaping Cerrado fire regimes, with profound implications for biodiversity conservation, ecosystem resilience and carbon cycling in tropical savannas, stressing the need for fire management policies that differentiate between traditional, prescribed and agricultural ignitions.

Keywords: neotropical savannas, fire regimes, fire ignitions, lightning, anthropogenic fires

1 Introduction

Many ecosystems in the world co-evolved with fire and their flora developed a range of strategies to co-exist with this disturbance agent [1, 2, 3, 4]. These strategies include resisting fire; quickly resprouting, flowering, or germinating after fire; and even promoting fire occurrence by providing flammable biomass [5, 6, 7]. The ancient origins of such adaptations [6, 8, 9] indicate that fires, ignited primarily by lightning and volcanic activity, were common on Earth long before the appearance of hominids [10]. These fires contributed to the spread of ecosystems with sparse tree canopies in seasonally dry climates, giving rise to the savanna biome [4]. Consequently, some present-day fire-adapted ecosystems rely on a certain fire regime to maintain their open physiognomies [11, 12]. The appearance of humans, and particularly their acquired ability to use fire, further shaped fire regimes and ecosystems globally [4, 13]. Despite these early contributions, rapid human transformations of many processes and components of the Earth system have altered fire regimes [3], with profound consequences for many ecosystems [14] and biogeochemical cycles [15, 16].

Fire regimes are directly and indirectly influenced by human activities [17] through changes in ignition patterns [18, 19], landscape fragmentation [13], active fire suppression [20], and anthropic climate change [21, 22]. Humans ignite fires for many reasons, including agriculture and landscape management (both modern and traditional practices), deforestation, accidents or arson [17]. Today, humans and lightning are the primary drivers of fire activity on Earth [23]. Even though lightning densities over land are highest near the Equator and greatly decrease towards the poles [24], lightning is the main cause of fire in the remote boreal regions [25], while humans are considered to be the main cause of fires in the tropics, both in fire-adapted

ecosystems like grasslands and savannas [13, 26], and fire-sensitive ecosystems like rainforests [14].

Through ignitions, humans can expand the so-called fire niche to seasons and areas where lightning densities are low [18], as long as flammability conditions allow. That is, humans can shift the timing of fires towards drier [13, 27] or wetter [18] weather conditions than lightning fires, and broaden the geographical range of fire occurrence to landscapes with different characteristics (e.g. in terms of fragmentation or topography) [18]. Both these processes can give rise to fires with different behaviour (e.g. in terms of size and intensity) than naturally occurring fires [19]. In addition, humans can increase or decrease the frequency of fires in different ecosystems.

In the case of fire-adapted ecosystems, there is currently much debate about the impacts of both increased fire frequencies and the suppression of fires, since both can alter vegetation structure and biodiversity [28]. Quantifying how much the current patterns of human-ignited fires differ from those started by lightning can help clarify the potential impacts of human-modified fire regimes, and contribute to strategies and interventions that contribute positively to fire-adapted ecosystem processes, rather than perpetuating practices that increase pressures on these ecosystems. Further, isolating lightning fires can bring new insights into the fire regimes these ecosystems evolved with [13].

The balance between lightning and human fire ignitions is particularly relevant to the Brazilian Cerrado, the world's most biodiverse tropical savanna [29]. This region is formed by fire-adapted grasslands and savannas with different levels of canopy cover intermingled with patches of riverine forests where fire-sensitive species are present [30]. Such diversity is argued to stem from nearby ecosystems evolving adaptation strategies to fire [6, 31], which, together with the stochastic nature of fire and factors such as soil composition [32], contributed to creating the mosaic of vegetation that characterises the Cerrado [33]. In addition, studies on the use of fire by indigenous peoples indicate that, over millennia, different communities developed a refined knowledge of fire management [34, 35, 36, 37] that may have further contributed to the Cerrado's heterogeneity [38, 39, 40]. In these traditional patch mosaic burning practices [34], fire is used with varying frequencies, and at different times throughout the dry season for a range of purposes, including regenerating pastures, clearing vegetation for cultivation, hunting and landscape management [36, 37, 41].

Today, industrial agriculture is the main economic activity in the Cerrado, producing both livestock and commercial crops like soybean and sugarcane [42]. This economic transformation has been particularly acute over the past few decades, when over 50% of the Cerrado's native vegetation has been lost to land use changes [43]. The current patterns of fire in this region clearly reflect this expansion [44, 45, 46], with reduced fire activity in highly converted areas where humans can exert strong controls on fire and vegetation is highly fragmented, and increases associated with human activities and climate change where the Cerrado has remained more intact [44, 45, 46, 47]. Humans are considered to be the main cause of fire

ignitions in the Cerrado given the widespread presence of modern agricultural activities and their concomitant use of fire [33, 48]; the high fire frequencies observed in some areas [46]; the disproportionately larger percentage of human fires compared to lightning fires in nearby ecoregions like the Pantanal [27]; and the mismatch between the fire season and the lightning season [49].

Lightning activity in the Cerrado changes throughout the year in accordance with precipitation patterns [49]. The highest incidence of lightning strikes occurs during the wet season (October to April) and the lowest during the dry season [49], when most fires take place [50]. Still, some early studies in protected areas of the Cerrado suggested that lightning strikes are a prevalent cause of fires [51, 52, 53], noting that lightning strikes can ignite fires even during the wet season causing generally small and patchy fires that are quickly extinguished by rainfall [51]. Despite these observations in protected areas, to our knowledge there has been no formal assessment of fire ignition causes across the whole Cerrado.

Here, we use geospatial data on individual fire perimeters from the Global Fire Atlas (GFA)[26, 54] and lightning occurrence from the Vaisala GLD360 dataset, along with an ignition-cause attribution method [55], to identify fire events in the Cerrado most likely to be caused by lightning strikes or by humans from 2019-2023. First, we aim to quantify the proportion of lightning and human-caused fires and study how these change throughout the year. Then, using an equal-area 30 km grid, we quantify the spatial patterns of lightning and human-caused fires to identify areas of the Cerrado potentially dominated by a particular ignition cause. We complement these analyses and their interpretation exploring the patterns of lightning activity during the year and their relation with rainfall, and across the Cerrado. Finally, we compare the fire frequencies of both ignition types, and their fire behaviour in terms of size and Fire Radiative Power (FRP) - a proxy for fire intensity - in relation to the level of human presence in the landscape and the weather conditions at ignition. We expect current Cerrado fire regimes to be dominated by human-caused fires, and for these fires to present more extreme behaviour than lightning fires, as previously suggested [51, 53, 56].

2 Results

2.1 Quantifying lightning and human-caused fires

We estimate that, in the period 2019-2023, 7.5% (95% CI, (6.0, 9.0)%) of all fires in the Brazilian Cerrado were ignited by lightning, 89.1 % (95% CI, (86.9, 91.3)%) were ignited by humans, and the remaining 3.4% (95% CI, (2.7, 4.1)) had no clear ignition cause. Similarly, around 7.9% (95% CI, (5.6, 10.4)%) of the annual burned area was caused by lightning fires, 88.7% (95% CI, (85.3, 92.0)%) was caused by humans, and 3.4% (95% CI, (2.4, 4.4)%) had no clear ignition cause.

Exploring these percentages by year, we observed some inter-annual variability both in

the number of lightning fires and in the burned area associated with this type of fire (Figure 1). The year 2021 had the lowest percentage of lightning fires, 6.5 (95% CI, (6.0, 7.0)%), and smallest burned area caused by lightning, 5.8% (95% CI, (5.2, 6.4)%); while 2023 had the highest values, 10.1% (95% CI, (9.3, 11.1)%) and 11.7% (95% CI, (10.7, 12.8)%), respectively.

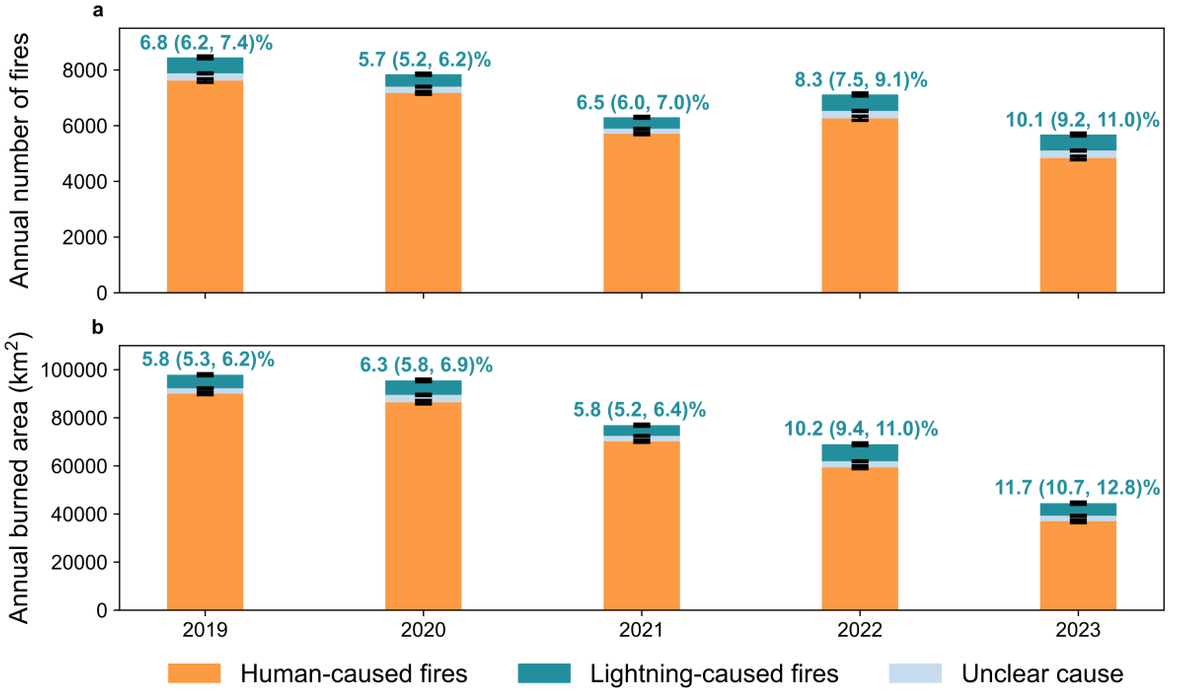

Figure 1: **Annual number of fires and burned area per ignition cause in the Brazilian Cerrado between 2019 and 2023.** Inter-annual variability throughout the study period (2019-2023) of the, **a**, number of fires caused by humans (orange) and lightning (blue), or with no clear cause of ignition (grey), and the corresponding annual burned areas, **b**. Numbers indicate the percentage of fires ignited by lightning in the year (**a**), and the percentage of burned area from lightning fires (**b**). Error bars indicate the 95% confidence interval (CI).

Most lightning fires occurred during the transition from the dry to the wet season, in September and October (Figure 2 a). While the lightning-fire season was concentrated in these two months - and to a lesser extent in November -, the human-caused fire season commenced earlier, spanning from May to October, and peaking in August and September (Figure 2 a).

Quantifying the balance between lightning and human-caused fires in each month, we observed that the dry season was clearly dominated by human fires, which caused more than 80% of fires from May to October (Figure 2 b). In contrast, during the wettest months (December to February) the percentage of lightning fires was similar or even larger than that of human fires, albeit the number of GFA fire perimeters was remarkably low during this period (Figures 2 a and b). October was the month with the highest number of lightning fires, which accounted for 20.9% (95% CI, (13.9, 27.7)%) of fires, while in September this percentage was

only 8.1% (95% CI, (2.6, 13.6)%). Finally, July was the month with the lowest percentage of lightning fires, which caused less than 1% of fires.

Because lightning occurs predominantly over the wet season (Figure 2 d) and is often accompanied by rainfall, we might expect a large share of lightning-ignited fires to be among the small fire sizes. However, coarse burned area products - like MCD64A1 [57] on which the GFA is based - have high omissions errors among small fires [58, 59]. To assess this source of uncertainty, we explored how the proportion of lightning fires changes when gradually removing the smallest sizes. We found that the proportion of lightning fires increased rapidly from around 7.5% when including all fires, up to around 8.2% when excluding fires smaller than 500 ha (Supplementary Figure 1), indicating we might be underestimating lightning fires. However, this change in the proportion of lightning fires lies within the 95% confidence interval estimated for the total proportion of lightning fires.

2.2 Spatial patterns of lightning and human-caused fires across the Cerrado

Using an equal-area 30 km grid over the Cerrado, we estimated the proportion of fires per ignition class for each grid cell to understand how fire-ignition patterns changed across the study region between 2019 and 2023. We found considerable overlap between the areas where most lightning and most human fires occur (Figure 3 a and b). However, there was a notable exception to these overlapping patterns in the northern ecoregion of Alto Parnaíba [60], where fires were predominantly caused by human ignitions, which caused more than 90% of fires (Figure 3 d). Nonetheless, in general, the Cerrado's fire regimes were dominated by anthropic fires, as humans were the main ignition cause of fires ($\geq$ 50%) in 94.5% of the grid cells with more than 10 fires on average in the study period (Figure 3 d). In this part of the analysis (Figure 3 d), we excluded those cells that experienced less than 10 fires in total over the period to prevent results that may not be representative of ignition dynamics but rather capturing noise. The excluded cells were concentrated in the south of the Cerrado (Figure 3 d) where landscapes are highly fragmented and usually present fewer and smaller fires, associated with longer human occupation and controls on fire [44, 61], but which are also prone to larger omission errors [62].

The percentage of lightning fires across grid cells ranged from 0 to around 60%, and only less than 2% of the Cerrado presented percentages above 40%. In general, the average number of lightning fires per year was small, around 4 fires in the grid cells with the highest occurrences. Lightning fires were concentrated in the ecoregions of the Bananal, the west of the Araguaia-Tocantins, and the northwest Planalto Central [60] (Figure 3 a). The southern parts of these ecoregions presented the largest percentage of lightning fires (Figure 3 d).

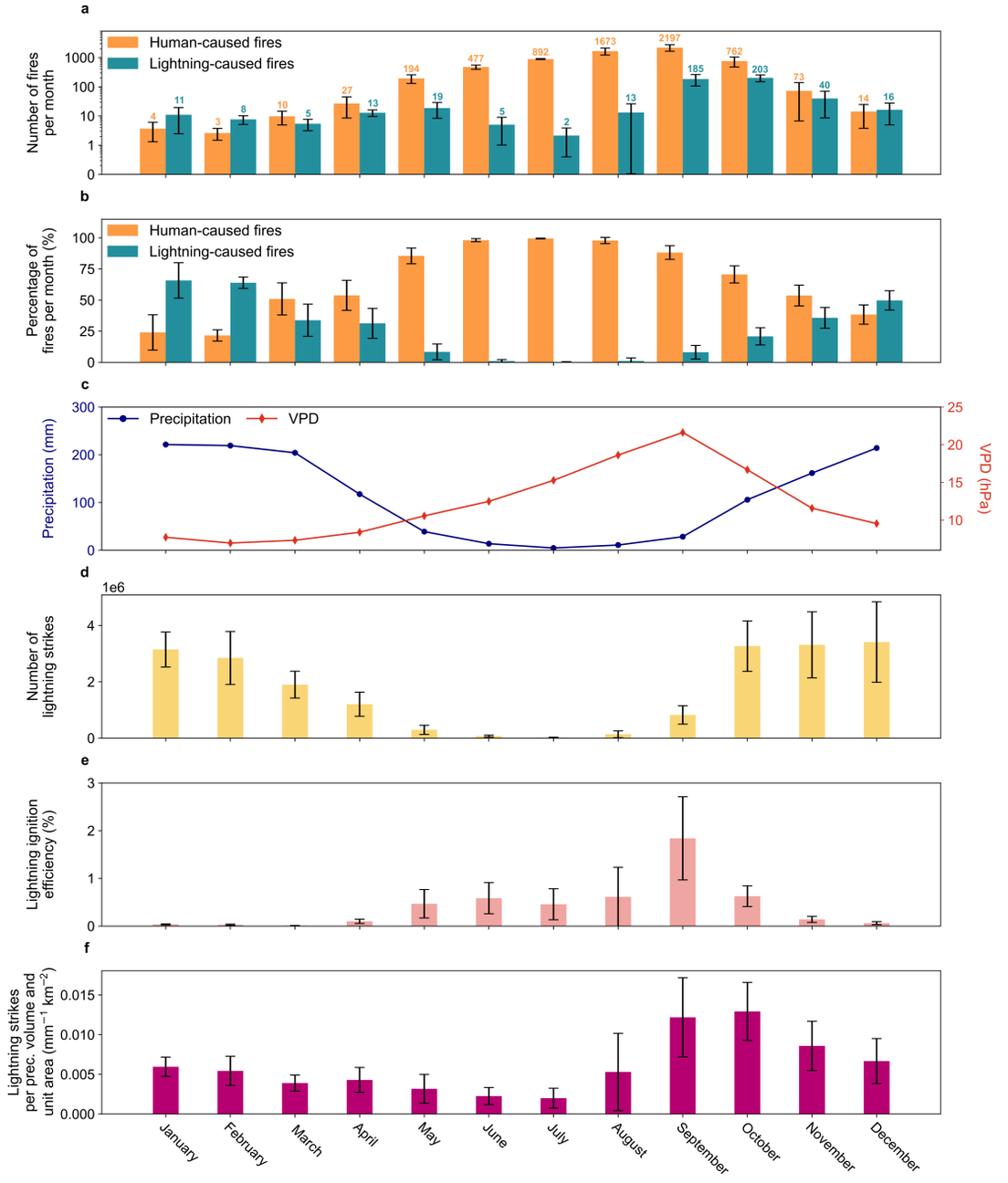

Figure 2: **Intra-annual patterns of the number of fires, climatic conditions and lightning activity. a** Average number of human-caused (orange) and lightning-caused (blue) fires per month in the study period, 2019-2023, also indicated with numbers. Note that the y-axis is in log-scale so that all colour bars can be clearly seen, but that there are some differences of up to two orders of magnitude. **b** Average monthly percentage of fires for each type of ignition. Lightning and human-caused fire percentages in each month do not necessarily add up to 100% as there can be fires with no clear ignition cause (see Methods). **c** Average monthly precipitation (blue) and VPD (red). **d** Average number of lightning strikes per month. **e** Lightning ignition efficiency, the number of lightning strikes igniting fires divided by the total number of lightning strikes. **f** Number of monthly lightning strikes per unit area and per unit monthly precipitation volume. Error bars were obtained from the standard deviation and represent the 95% confidence interval (CI).

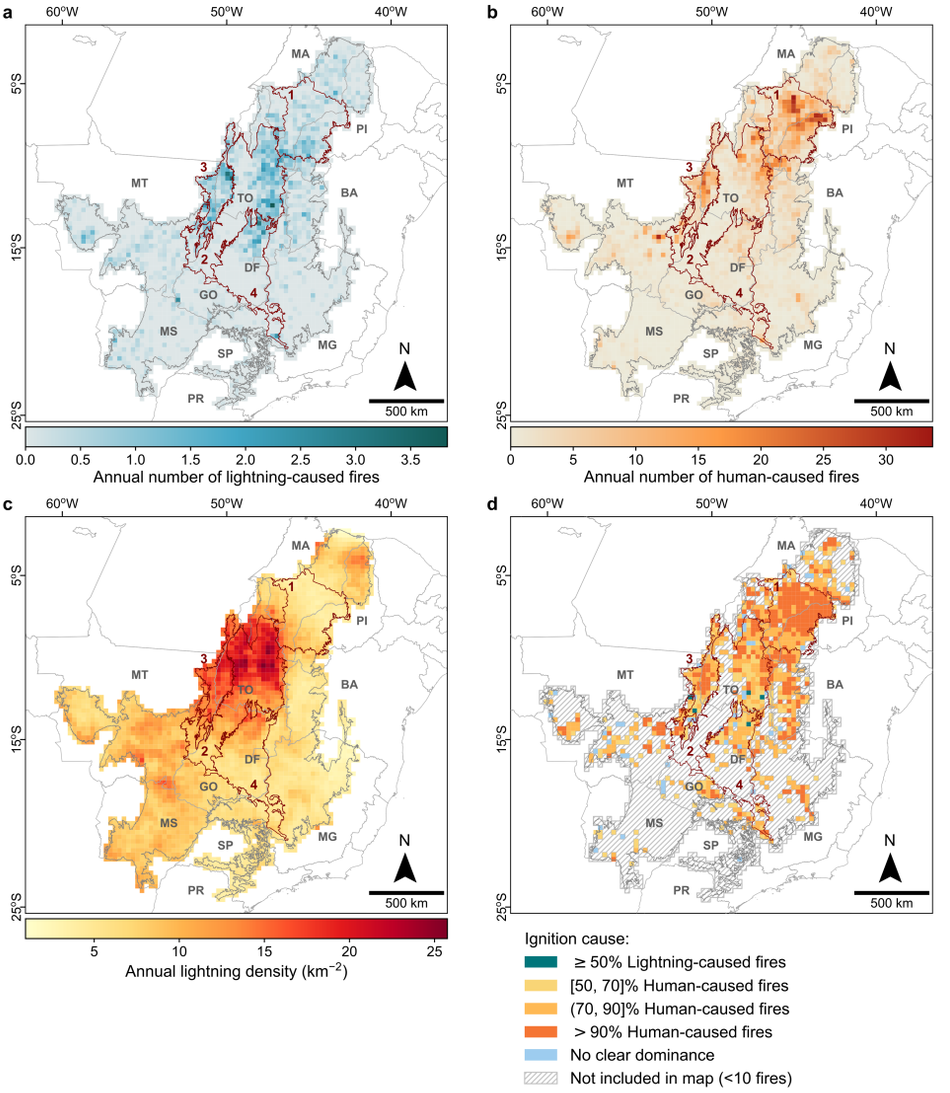

Figure 3: **Spatial patterns of fire activity by ignition type and lightning activity across the Brazilian Cerrado.** Average annual number of **a** lightning and **b** human-caused fires, and **c** lightning density in each 30-km cell over the Cerrado in the period 2019-2023. Note that maps **a** and **b** have different scales so that the spatial variation in the number of lightning-caused fires is visible despite its numbers being overall much smaller than those of human-caused fires. **d** map showing the grid cells dominated by lightning (blue) or human ignitions (yellow and oranges), that is, where one of the two causes of ignitions accounts for 50% or more of ignitions in a grid cell. Grid cells coloured in pink do not have an ignition cause accounting for more than 50% of fires (as there are fires with no clear ignition cause). Cells with less than 2 fires on average per year (less than 10 in the period). Areas and numeric labels highlighted in red correspond to the Cerrado ecoregions referred to in the text: 1, Alto Parnaíba; 2, Araguaia Tocantins; 3, Bananal; 4, Planalto Central. Grey labels indicated the Brazilian states intersecting the Cerrado: MT, Mato Grosso; MS, Mato Grosso do Sul; GO, Goiás; DF, Distrito Federal; SP, São Paulo; PR, Paraná; MG, Minas Gerais; MA, Maranhão; TO, Tocantins; PI, Piauí; BA, Bahia.

2.3 The spatiotemporal patterns of lightning

We observed a strong temporal co-occurrence of precipitation and lightning (Figures 2 c and d), as expected. Accordingly, in the middle of the dry season, from June to August, the number of lightning strikes was lowest, while they were highest during the wet season, December to February. In fact, there were 100 times more lightning strikes during the later period than the former. However, the lightning ignition efficiency was highest from May to October (between 0.5 and 1.8%, Figure 2 d), while from December to March only about 0.04% of lightning strikes ignited fires.

Interestingly, September and October were the months with the largest numbers of lightning strikes per unit area and per unit volume of precipitation (Figure 2 e), precisely when the number of lightning-caused fires peaked. That is, during the transition from the dry to the wet season, when the first rains begin but the monthly precipitation has not yet reached its peak, there is a higher number of lightning strikes per precipitation volume compared to the rest of the year.

Lightning strikes were not uniformly distributed across the Cerrado (Figure 3 c). In particular, the state of Tocantins presented the highest levels of lightning density, along with the northern parts of Mato Grosso and the north of Goiás, in the centre-west of the Cerrado. The state of Mato Grosso in the south-west, and the north-eastern tip of the Cerrado experienced intermediate levels of lightning activity. In contrast, the south-eastern regions of the Cerrado along with an area roughly corresponding to the Alto Parnaíba ecoregion [60] in the north presented the lowest levels of lightning densities, about ten times fewer strikes than the grid cells with highest levels. Finally, during the dry season and particularly in June, many areas of the Cerrado experienced no lightning strikes - especially in the centre, while the southern- and northern-most parts of the Cerrado did experience some level of lightning activity throughout the year (Supplementary Figure 2).

2.4 The fire frequencies of lightning and human-caused fires

Comparing the fire frequency distributions of lightning and human-caused fires (Figure 4) - that is, the distribution of the number of times a certain grid cell burned in relation with each ignition cause (see Methods) -, we found that most of the area affected by fire over the 5 years of the study period burned only once for both types of ignition. However, around 28% of the areas affected by human-caused fires burned two times or more, while only about 6% of the areas affected by lightning burned more than once. Furthermore, the areas that that experienced lightning-caused fires four times was very small (3 km^2, $\simeq 0.01\%$) and none burned five times. In contrast, around 3,550 km^2 were affected by human-caused fires four times ($\simeq 1.4\%$ of the human-affected area), and 1,190 km^2 ($\simeq 0.5\%$) burned every year between 2019 and 2023.

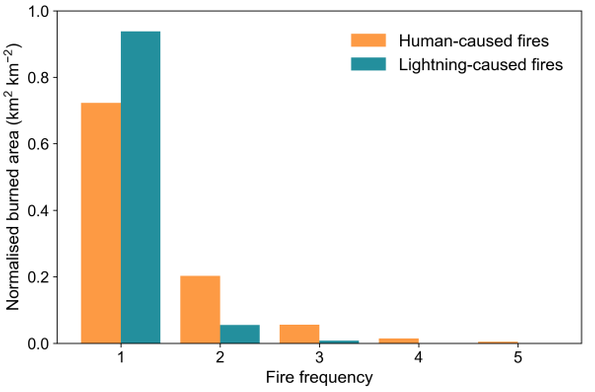

Figure 4: **Fire frequency per ignition cause.** Fire frequency distributions for lightning-caused (blue) and human-caused (orange) fires in the period 2019-2023. Bars represent the areas burned by each type of ignition a certain number of times in the study period divided by the total area affected at least once by that ignition class.

2.5 Comparing weather conditions and landscape characteristics

Fire occurrence and behaviour for both lightning and human-caused ignitions are shaped by the environmental conditions under which fires occur. We therefore investigated weather conditions at the time of ignition — governing fuel flammability [7]— and landscape fragmentation — constraining fuel continuity and fire spread — for both ignition sources.

Lightning-ignited fires took place in more humid conditions than human-ignited fires, with overall larger accumulated precipitation (over the 10 days prior to ignition, see Methods) and lower VPD values at ignition (Figure 5 c and d). Importantly, we observed these same patterns when comparing by month (Figure 5 a and b), with particularly acute differences from August to October.

We also explored how fire density (number of fires per unit area) for both ignition causes and lightning density changed with the level of landscape fragmentation, which we estimated as the percentage of non-anthropogenic land cover area (hereafter, unconverted or natural area, see Methods and Supplementary Figure 3). We found that, even though lightning density was similar across levels of natural area - meaning there was a similar number of lightning ignition opportunities across fragmentation levels -, the number of lightning-caused fires detected increased with the percentage of unconverted or natural area (Supplementary Figure 3 b). Similarly, the number of human-caused fires detected increased towards less converted landscapes (Supplementary Figure 3 a). Hence, most fires occurred in landscapes with lower levels of conversion and fragmentation ($\geq$ 60% of natural area) for both ignition causes.

Finally, we also explored the distances from each ignition point to the nearest road and urban area, as well as for a subset of 500,000 lightning strikes selected at random (in the interest of computational time). We found that the distance distributions for these three types of events were skewed towards small values (Supplementary Figures 4 a and c). That is,

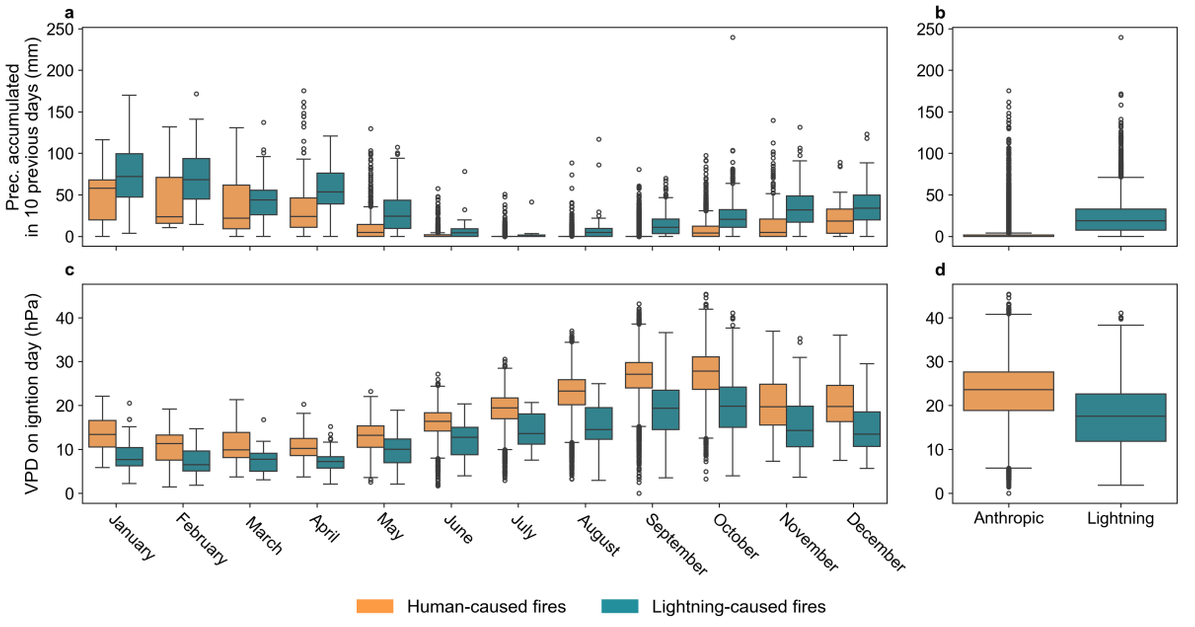

Figure 5: **Monthly weather conditions at fire ignition per ignition cause. a**, distribution of the precipitation accumulated over the 10 days prior to the fire start per month for lightning (blue) and human-caused (orange) fires, and, **b**, over the study period 2019-2023. **c**, distribution of VPD values on the day of ignition per month, and, **d**, over the whole period, per ignition cause.

the proportion of fires (both lightning and human) and lightning strikes happening at shorter distances was larger than the number of fires and strikes occurring further away. Still, we did observe that the distribution of distances for human-caused fires appears slightly more skewed towards small values than that of lightning-caused fires (Supplementary Figure 4). However, the most remote human-caused and lightning-caused fires started at similar distances from roads (Supplementary Figure 4).

2.6 Comparing fire behaviour in relation to ignition cause

The distributions of fire size and median FRP of lightning and human-caused fires did not present substantial differences in terms of the medians (Figure 6 and Supplementary Figure 5) . However, there were remarkable differences in the largest values of both fire behaviour variables. For example, the largest human-caused fires were about one order of magnitude larger than the largest lightning-caused fires (Figures 6 b), and the largest median FRP values were about two times larger (Figure 6 d).

Differences in fire sizes between lightning and human-caused fires were conditional on the timing of fire ignition. The largest human-ignited fires occurred in August (Figure 6 a), when the difference between largest sizes was also greatest; followed by September, when the largest lightning fires were closer in size to the human-caused ones. In contrast, we did not observe remarkable differences between the largest sizes of the two types of fires in October nor during

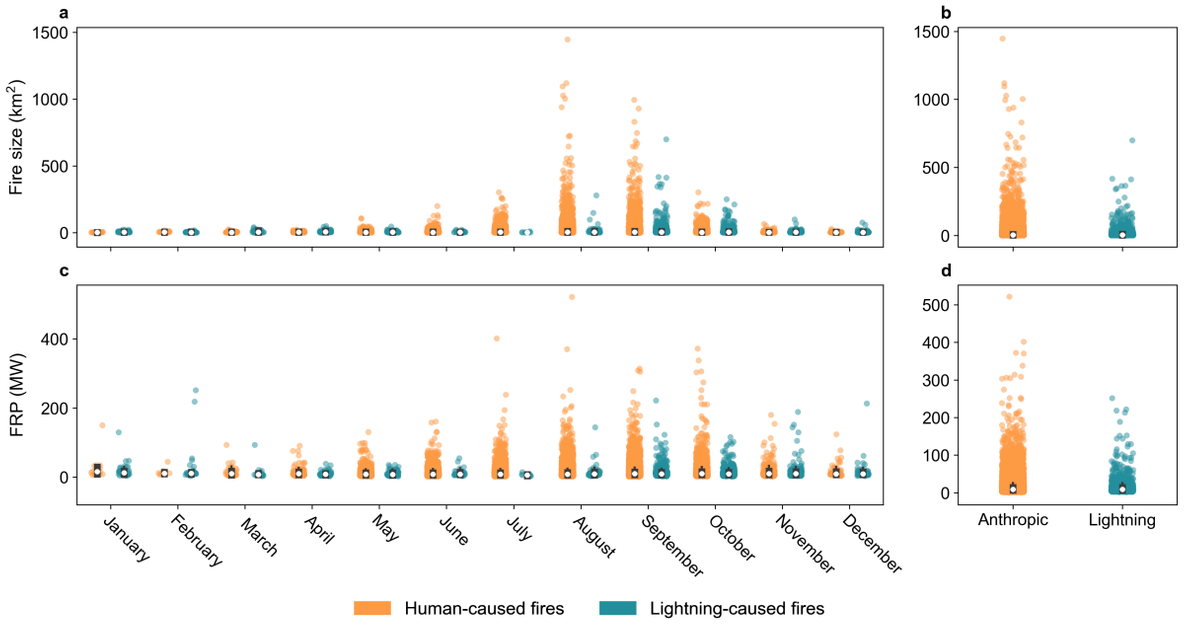

Figure 6: **Monthly fire behaviour per ignition cause.** Distribution of the fire sizes and median fire radiative power (FRP) of lightning (blue) and human-caused (orange) fires. The distributions are shown as a stripplot of the observations - that is, each orange or blue dot in the graph represents a fire event. The white dots represent the median value of each distribution, and the black box-and-whisker show the quartiles of the distributions. **a** and **c** show the distributions per month for fire size and median FRP respectively. **b** and **d** show the fire size and median FRP distributions over the period 2019-2023 respectively.

the wet season (Figure 6 a).

Regarding FRP, we observed similar seasonality patterns (Figure 6 c), with generally small values during the wet season for both types of fire. The most intense human-caused fires took place in the dry season, while the most intense lightning fires occurred in the dry-wet transition period. Again, human-caused fires had higher FRP values than lightning ones during these periods, while they were overall similar during the wet season.

Lastly, we explored the weather conditions and landscape characteristics of the largest ($\geq$ 150 km^2) and most intense ($\geq$ 100 MW) fires (Figure 7). We found that the largest human-caused fires took place in less fragmented landscapes ($\geq$ 80 % natural area) and in the driest conditions (Figures 7 a and b, and Supplementary Figure 5 a). In contrast, the largest lightning fires were more spread out across landscapes ($\geq$ 50 % natural area) and practically all of them occurred in areas that had experienced some rainfall in the days before the fire (Figure 7 a). In addition, the largest lightning fires occurred in lower VPD conditions than human ones (Figure 7 b). Regarding FRP values, the most intense fires were spread out across all levels of fragmentation (Figures 7 c and d, and Supplementary Figure 5 b), and the most intense human-caused fires took place in drier and hotter conditions than the most intense lightning fires.

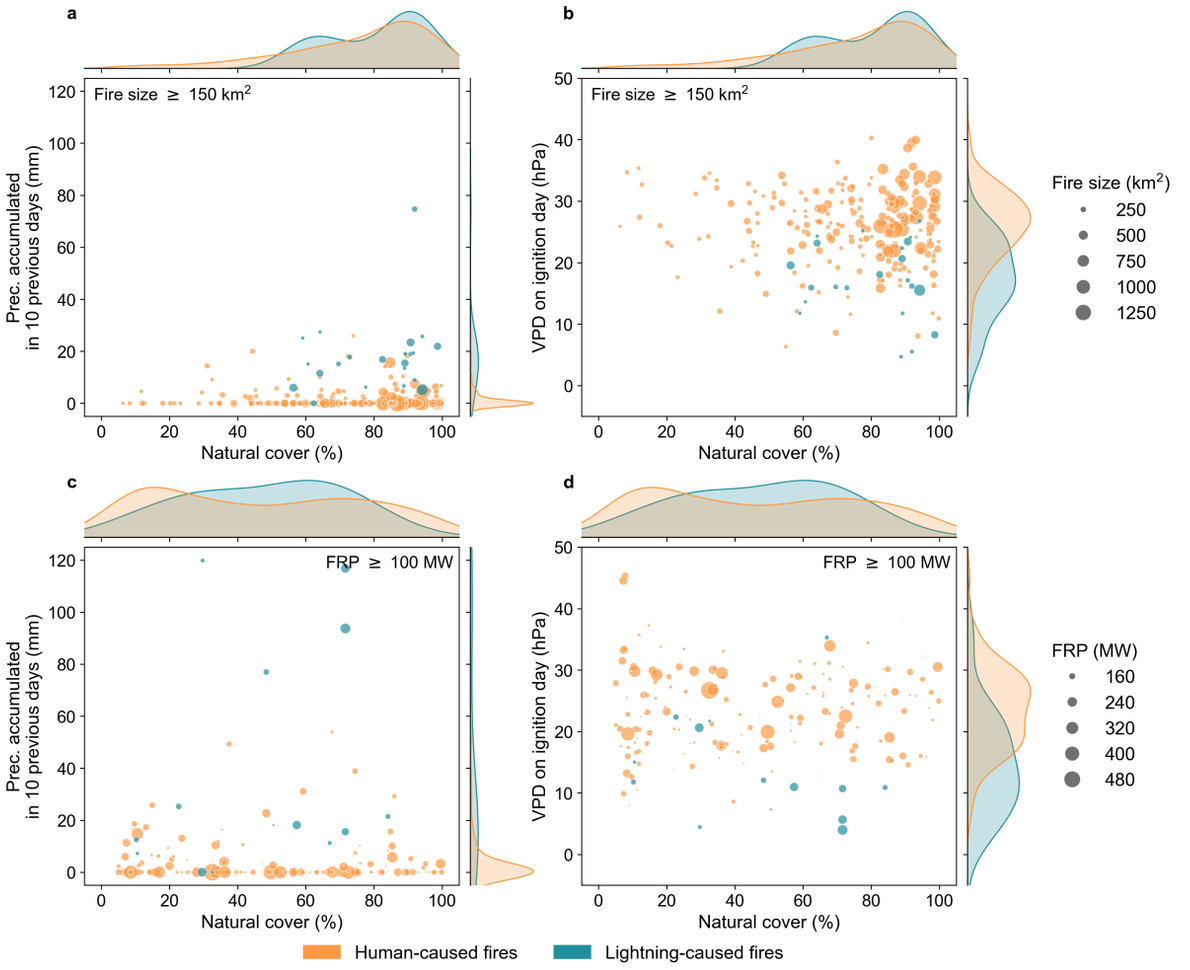

Figure 7: **The environmental conditions of the largest and most intense fires per ignition cause.** Weather conditions and natural area percentage of the ignition points of the largest ($\geq$ 150 km^2) fires (top row) and the most intense (median FRP $\geq$ 100 MW) fires (bottom row). Each dot represents a fire observation coloured by type of ignition, either human-caused (orange) or lightning-caused (blue). The size of the dot represents the size (top row) or the median FRP value (bottom row) of the fire. **a** and **c**, show the relation between the precipitation accumulated in the 10 days prior to ignition and the percentage of natural area of the cell where the fire took place for the largest and most intense fires respectively. **b** and **d**, show the relation between the VPD conditions on the day of ignition and the percentage of natural area for the largest fires and most intense fires respectively. In each plot, the top and right panels represent the density of occurrences for the corresponding variable (these density plots are not normalised so that the distribution of the lightning-caused fires, which have much lower numbers, can be observed).

3 Discussion

Across the Brazilian Cerrado, an estimated 7.5% (95% CI, (6.0, 9.0)%) of all fire ignitions was caused by lightning in the period 2019-2023, while human activities were attributed 89.1% (95% CI, (86.9, 91.3)%) of fire ignitions - be it for agricultural purposes, for native vegetation conversion, as part of fire management practices or accidentally -, and 3.4% (95% CI, (2.7,

4.1)%) did not have a clear ignition cause. Our findings highlight the extent of the human footprint on the Cerrado's current fire regimes and how these substantially differ compared to lightning-caused fire regimes. Indeed, we found that human ignitions dominate across the Cerrado, as they account for more than 50% of fires [18] in over 90% of its area (Figure 3 d). Further, we showed that humans lengthen the fire season three-fold and shift it towards the dry season, when vegetation is abundant after the growing period [63] and weather conditions are dry (Figure 2 a and c), but natural ignitions are rare due to low lightning occurrence (Figure 2 d). Therefore, humans would be extending the fire season by creating ignition opportunities throughout the dry season, when fuel load and flammability conditions are favourable to fire spread [64]. Moreover, we found that humans are the cause of the largest and most intense fires (Figure 7), with extreme fire behaviour that is not observed amongst the fires ignited by lightning. These differences may be related to lightning often being accompanied by rainfall and moist weather conditions that prevent extreme fire behaviour, unlike human ignitions (Figures 5 and 7).

We estimated that most lightning-caused fires, around 75%, took place in the transition period from the dry to the wet seasons (September and October, Figure 2 a), in agreement with previous studies in different areas of the Cerrado [49, 51, 53, 56, 65], while they were much lower during the core months of the dry and wet seasons. The trade-off between vegetation dryness and the occurrence of sufficient lightning ignition opportunities enabling the fire seasons [2] may explain these temporal patterns. The moisture content of the vegetation diminishes throughout the dry season and larger ratios of biomass become flammable [66], explaining the higher lightning-ignition efficiency observed during the dry season (Figure 2 d), as noted in other ecosystems [67]. However, the density of lightning strikes from June to August is very low (Figure 2 c) - precisely due to the lack of atmospheric events leading to cloud formation -, possibly acting as a limiting factor to the occurrence of lightning-ignited fires. Conversely, during the wet season, lightning density is high (Supplementary Figure 2), but high precipitation and low VPD impair fuel flammability, thus limiting fire occurrence regardless of ignition cause (Figure 2 a). However, the quantification of fires during this period must be considered with care because wet-season fires tend to be small, patchy and of low intensity [51, 53, 56], and the cloud cover much denser, making them less likely to be identified in satellite-based burned area products [62, 68]. Therefore, our results seemingly underestimate the amount of fires occurring during the wet season, a period during which studies in different Cerrado protected areas and other savanna-like ecosystems have observed numerous lightning fires [27, 51, 53, 56]. In the dry-to-wet transition periods, however, we observed that lightning density increases as rainfall restarts, while precipitation has not yet reached maximum levels and VPD is still high (Figure 2 c), so large amounts of fuel may still have low moisture content. In addition, we find a larger ratio of lightning strikes per precipitation volume in September and October (Figure 2 e). This confluence of factors can explain the higher incidence of lightning fires in this period.

The majority of fires, however, are caused by humans and take place over a longer period (May to October), precisely during drier months (Figure 2 a and c), as suggested in previous studies [44, 48, 50, 69]. This shift in the fire seasonality implies that Cerrado vegetation could be experiencing fires in a phase of the phenological cycle that may not correspond to the timing of fire it co-evolved with [63]. Further, human-caused fires present higher fire frequencies when compared to lightning-ignited fires (Figure 4), possibly reflecting the use of fire in modern agricultural practices to burn residues or renew pastures that will repeatedly affect the same areas [48]. In contrast, the stochastic nature of lightning strikes and the necessary co-occurrence with appropriate flammability conditions may limit the probability of high frequencies associated with lightning-caused fires. The seasonality mismatch, combined with the higher fire frequencies of current human ignitions may eventually lead to negative impacts on native vegetation even if adapted to fire [70], particularly in the context of climate change.

The characteristic vegetation mosaic of tropical and subtropical savannas, with low to intermediate levels of tree cover, is promoted by certain disturbance regimes that maintain these ecosystems' structure [71, 72]. As such, intermediate fire frequencies in-between seasons are argued to promote sufficiently open ecosystems with abundant ground flora [70], while allowing some trees to escape the fire trap and sustain a certain tree cover level [11]. Evidence shows that very frequent dry season fires - around every one or two years - can disrupt the fire-mediated stability [70] because they increase vegetation mortality, even when adapted to fire, hampering tree recruitment and reducing aboveground biomass [73]. As such, if prolonged over time, the shifts in the seasonality of fires and the exacerbated frequencies created by humans could be promoting degraded or alternative treeless states [72]. Still, albeit not described in this study, humans are also known to have altered Cerrado's fire regimes by diminishing fire frequencies through active suppression, particularly in some protected areas [40, 74]. Such fire regimes contribute to shifting savannas' vegetation towards more closed canopy states [75], with lower biodiversity [28, 74] and higher risk of larger and more intense fires [40].

We can expect both these processes of change to be further reinforced by climate change. On the one hand, the dry season of the Cerrado has lengthened over the past few decades as a consequence of the changing climate [22], thus expanding the window of readily flammable fuel. On the other hand, the increased drying capacity of the air (i.e. VPD) caused by rising temperatures can make vegetation prone to fire more easily [64], including Cerrado physiognomies that are not typically affected by fire (e.g. patches of forest formations) [40]. As such, climate change would be expanding the climatic niche of fire occurrence by increasing the likelihood of fire throughout the year and across vegetation formations [64], which could further couple with human ignitions and the potential ecological effects of human-created fire regimes.

Using accumulated precipitation and VPD on the day of ignition as proxies for fuel moisture

content [76, 77], we found that even when occurring in the same month, human-caused fires tend to take place in drier and hotter conditions than lightning-caused fires (Figure 5). These differences emphasise the fact that human ignitions are less constrained as they only require that fuels are sufficiently flammable and continuous, while lightning ignitions tend to co-occur with rainfall events even during the dry season [49]. In addition, the remarkable differences in weather conditions at ignition during the transition period also suggest that humans may have a tendency to target drier weather, especially when fire is set to fulfill a purpose [48].

Analogously, human ignitions seem to be less constrained geographically than lightning ones. We found that humans are the main cause of ignition across most of the Cerrado (Figure 3 d), even starting fires at long distances from roads and urban areas (Supplementary Figure 3). In particular, we found a continuous region in the north of the Cerrado strongly dominated by human ignitions (causing $\geq$90% of fires, Figure 3 d), corresponding to the ecoregion of Alto Parnaíba [60]. This area presents a comparatively low number of lightning-caused fires, possibly limited by the also comparatively low density of lightning strikes (Figure 3 c). Furthermore, the Alto Parnaíba is found within the so-called Matopiba region, which is considered the Cerrado's last agricultural frontier. This region has experienced large-scale native vegetation conversion over the past two decades [42, 78], where fire is often used in relation to agri-business activities - particularly for vegetation conversion [79, 80].

Nevertheless, we found that both lightning and human-caused fires are similarly concentrated in areas with larger native vegetation remnants, while both types of fires are low in highly fragmented areas (Supplementary Figure 3). Such patterns indicate that the spatial distribution of fires in the Cerrado may be more dependent on bioclimatic and landscape factors, as previously suggested [44, 45, 46, 69]. Highly fragmented areas are mostly concentrated in the south of the Cerrado [43] and correspond to consolidated land-use areas where people tend to exert strong controls on fire and vegetation, which can explain the lower ratios of human and lightning fires. In contrast, unconverted areas in the Cerrado are mostly under great pressure from land conversion, which usually involves the repeated use of fire [80, 81]. Still, satellite burned area products with coarse resolution, such as MCD64A1 from which the GFA is derived, can only capture fires larger than a certain size (around 0.21 km^2 in the GFA) and have high omission errors in agricultural landscapes of Cerrado where fires tend to be small and their spectral signal can be confounded [58, 62]. For example, using a higher spatial resolution (20 m) burned area product, Ramo et al. [59] found that in Sub-Saharan Africa, small fires ($<$ 100 ha) make up 41% of total burned area but only 4.9% in the GFA product, which maps 16 times less burned area from small fires [59]. Hence, considering such findings, we may be underestimating the burned area from small fires ($<$ 100 ha) by more than one order of magnitude (Supplementary Figure 1 a), while large fires ($>$ 500 ha) are mapped with fewer omissions by coarse burned area products [59] with about 80% accuracy over the Cerrado [58]. Further, since in tropical and subtropical savannas small fires occur in higher proportions during the transition periods [59], this underestimation is likely to be

higher than one order of magnitude during these periods. Because the omission of small fires might particularly affect lightning fires, we calculated the changes in the proportion of lightning fires as we gradually removed small fires. While the proportion increased removing fires up to around 500 ha indicating we might be underestimating lightning fires due to small fire omissions (Supplementary Figure 1 b), this change of 1% is within the estimated confidence level (6-9%). Additionally, the lightning strikes dataset is based on a network of ground-based sensors that may contain omission errors, further contributing to the potential underestimation of lightning-ignited fires. Even though a formal assessment of the lightning detection efficiency and its spatial distribution was not available, the GLD360 lightning dataset has been reported to detect similar spatial patterns but orders of magnitude more lightning strikes than lightning sensors on-board satellites [82].

Comparing the fire behaviour of lightning and human fires, we found the most remarkable differences in the largest values of fire size and FRP distributions rather than in the medians, as observed in previous studies comparing fire behaviour for different fire categories [83]. For both types of ignitions, the largest and most intense fires are concentrated in the dry season (Figure 6) as expected [51], as this is the period when the vegetation is more flammable, giving rise to higher fire intensities and effectively extending the fuel bed continuity [17]. However, the largest ($\geq$150 km^2) and most intense ($\geq$ 100 MW) human-ignited fires occurred in overall drier conditions than their lightning counterparts (Figure 7). In both cases, the largest fires started in the least converted landscapes ($>$80% natural area, Figure 7), also as expected because land-use fragmentation exerts a strong control on savannas fire size through suppression and fuel discontinuities [17, 84, 85]. Therefore, the drier weather conditions at the time of the fire start may be a determining factor explaining the more extreme behaviour of human fires. Still, the final size and intensity of fires will also be influenced by the weather conditions over the course of the fire - which will possibly also be drier for human-caused fires as they are more concentrated in the driest months (Figure 2 a).

In comparison to lightning, humans expand the climatic and geographic niche of fire by creating ignitions in times of the year and regions where fires would otherwise be rare if solely ignited by lightning. These processes have been occurring since the first humans arrived in the Cerrado [86], and in other savannas and ecosystems [87]. Historically, human communities have used fire for different purposes and with different practices depending on the culture, and economic and governance systems [88], influencing the evolution of different ecosystems. However, not all uses of fire have the same effects on ecosystems and, therefore, some fundamental distinctions must be made between different uses, both historically and in the present. In the Cerrado in particular, there are differences between small-scale traditional uses of fires, the use of prescribed fires in integrated fire management (IFM) practices [89, 90], and those uses associated with modern agricultural activities [48, 91]. Indigenous peoples and pastoral communities in the first case, and environmental agencies and other organisations in the second, use mosaic burning practices where fire is planned and managed [36, 48]. These

practices intend to create landscapes of patches with different fire histories, which contribute to shaping and maintaining Cerrado's heterogeneous vegetation and biodiversity [38, 39, 40]. In modern agricultural uses, however, fire occurrence in native vegetation is usually a by-product of its use in the cultivation of commercial crops and cattle-ranching fields [48] or in native vegetation conversion [48, 81] and arson [53]. In these cases, fire is used with high frequencies, concentrated in the dry and late-dry season, and with little control on fire escape into adjacent native vegetation [48]. As such, we should expect different ecological impacts of fire on Cerrado ecosystems depending on the regimes that are created by different types of fire uses and landscape management. This study has aimed at quantifying and comparing lightning and human-created fire regimes solely, describing general patterns for each ignition source. However, the fire regimes created by different human communities and agents merit a detailed study, as the general scale and effects of these different regimes cannot be generalised. Future studies could further discriminate ignition cause amongst IFM, traditional practices, modern agricultural activities and lightning, to deepen our understanding about the fire regimes created in each case, their ecological effects, and how these effects may be impacted by climate change.

Our results highlighted the profound differences between the Cerrado's fire regimes caused by lightning and by human ignitions. We provided quantitative evidence that humans are the main cause of fires across the Brazilian Cerrado, creating an excessive number of ignitions and higher fire frequencies in comparison to lightning. We showed that lightning ignites a comparatively small but relevant fraction of fires, particularly in the transition period from the dry to the wet season, when adequate flammability conditions and high lightning densities concur. In contrast, humans lengthen the fire season by starting fires throughout the drier months of the year and in generally more flammable conditions than lightning, leading to more extreme fire behaviour. Further, we found that both types of fires are primarily concentrated in the least converted areas of the Cerrado, seemingly constrained by human controls in highly fragmented areas [44, 45, 46]. Therefore, our results indicate that, through fire ignitions, humans are altering the fire regimes of the largest remnants of Cerrado native vegetation towards more frequent fires and extreme behaviour than would naturally occur. Even though most Cerrado ecosystems are adapted to fire, the high frequencies of human ignitions may have negative impacts affecting the structure of the vegetation and leading to biodiversity losses [70]. These fire frequencies may particularly affect tree species by hampering tree establishment and promoting adult tree mortality [86], thus potentially affecting other species dependent on tree cover. However, more research must be devoted to understanding the complexity of the ecological effects of different fire regimes on Cerrado's ecosystems. In this sense, the recently adopted Brazilian National Policy on IFM (Lei n. 14,944) is a fundamental step forward as it not only establishes guidelines for IFM in fire-adapted ecosystems of Brazil, but it also regulates the use of fire for agricultural practices, as well as the unauthorised use of fire. Still, the extent to which the Cerrado has already been converted and its fire

regimes altered underscore the urgency and scale of conservation needed to protect this region. Therefore, it is crucial to enforce these promising policies with urgency and ensure that enough resources are allocated to implementing IFM and controlling the improper use of fire.

4 Methods

4.1 The study area

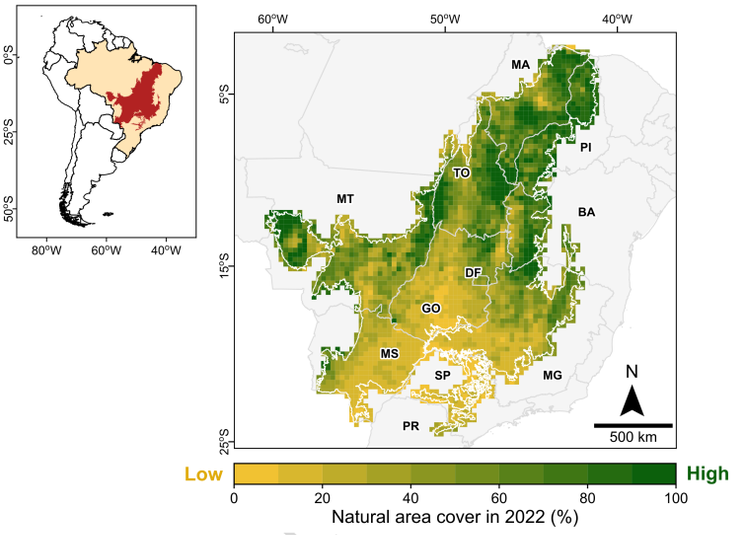

Figure 8: **The Brazilian Cerrado.** Location of the study area (left panel), the Brazilian Cerrado (red), within Brazil (yellow) in South America. The Brazilian Cerrado is coloured according to the natural area percentage of each 30-km grid cell in the year 2022 (right panel). We used land-use data from the MapBiomas Collection 8.0 [92] dataset. Values range from 0-10% natural area (orange), indicating cells mostly converted to human land uses, to 90-100% natural area (blue), indicating unconverted landscapes. Grey lines represent the limits of the Brazilian states, and the labels refer to states with some area in the Cerrado: MT, Mato Grosso; MS, Mato Grosso do Sul; GO, Goiás; DF, Distrito Federal; SP, São Paulo; PR, Paraná; MG, Minas Gerais; MA, Maranhão; TO, Toncantins; PI, Piauí; BA, Bahia.

The Brazilian Cerrado (Figure 8) extends over more than 2.2 million km^2, and is composed of very heterogeneous vegetation including primarily grasslands and savannas, but also forest patches [30]. The region stands out for its high levels of biodiversity and endemism [93], comprising fire-adapted species and, to a lesser extent, fire-sensitive species. This heterogeneity is reflected in the different ecoregions identified within the Cerrado [60]. The climate of the Cerrado presents a strong seasonality, with well-defined wet and dry seasons. Annual precipitation varies between 800 mm to over 1,800 mm roughly increasing from east to west [94]. Average annual temperatures vary between 18 °C and 28 °C, increasing along a latitudinal gradient towards the equator [94]. Lightning activity also presents a marked seasonality intimately tied to rainfall, with the density of both wet and dry lightning strikes peaking between November and March [49], the rainiest period over the Cerrado [94].

Currently, most of the Cerrado's original native vegetation has been converted to agricultural land uses, and ongoing conversion is still occurring in its northern half, the Matopiba region - comprising the Cerrado portion of the Brazilian states of Maranhão, Tocantins, Piauí and Bahía [78]. This ongoing large-scale conversion process in such a biodiverse region makes the Cerrado one of the world's biodiversity hotspots for conservation [95].

4.2 Data sources

4.2.1 Individual fire data

We used data on individual fire events from the Global Fire Atlas (GFA) [54], a global dataset derived from the Moderate Resolution Imaging Spectroradiometer (MODIS) MCD64A1 Collection 6.1 [57] burned area data with a daily frequency and 500-m spatial resolution. For the period 2002-present, the GFA provides information at the individual fire level in the form of georeferenced polygons representing the fire scar and the estimated coordinates of the ignition point, as well as the start and end dates of the fires, their duration, size, perimeter, average length of the daily fire line, and the rate and direction of spread.

To compare the fire behaviour of lightning and human-caused fires, we focused on the size and intensity of fires. The fire size was readily available from the GFA dataset, with a minimum fire size of 0.21 km^2 because of the MODIS spatial resolution. To study the intensity of fires, we combined the GFA data with active fire (AF) observations from the Visible Infrared Imaging Radiometer Suite (VIIRS) [96]. This instrument detects sub-pixel fire activity based on thermal anomalies with a daily overpass frequency and 375 m resolution [96] and provides fire radiative power (FRP), a measure of the radiative energy of the fire. As such, hereafter, we restricted our analysis to those GFA polygons overlapping with at least one VIIRS AF within a 375 m distance from the GFA perimeter and within the duration period of the fire indicated by the GFA. Next, we calculated the median FRP of each fire out of all the VIIRS AFs overlapping the polygon in space and time.

We used the coordinates of the ignition point and the estimated date of ignition to determine the plausibility that each fire perimeter was ignited by lightning (see Section 4.3.1). To estimate the date and location of the ignition point, GFA uses an algorithm that searches for local minima of the mapped burned dates of the MCD64A1 pixels within each fire perimeter [26]. As a consequence, the estimated date of ignition has an associated uncertainty between ± 1 day and ± 2 days [26, 97]. In addition, we estimated an upper bound for the uncertainty of the location of the ignition point to be around 2.2 km (Supplementary Figure 6 a). We estimated this uncertainty as the average maximum distance between the coordinates of the ignition point and the edge of the fire's sub-polygon formed by all pixels contiguous to the ignition point and with the same burn date - which was also provided by the GFA dataset [54]. Because lightning in the Cerrado usually occurs along with rainfall [49], most lightning-caused fires will ignite beneath clouds and will reach overall smaller sizes, which reduces their

detectability by satellite instruments. As such, it is worth noting that the uncertainty on the location and timing of lightning-ignited fires will probably be greater than that of human-ignited fires, and that the overall detection and identification of lightning-fires will possibly be underestimated.

4.2.2 Lightning data

We used lightning data from the Vaisala Global Lightning Detection Network GLD360, a global dataset on lightning strikes based on a network of lightning sensors. This network records the occurrence of lightning strikes, both cloud-to-ground and cloud-to-cloud, and provides information for each lightning strike: location, timing of occurrence and intensity. For the spatial uncertainty on the lightning ignition location, the dataset provides the angle and lengths of the semi-major and semi-minor axes of the confidence ellipse.

In this study, we used the GLD360 cloud-to-ground data on lightning strikes over the Cerrado for the period January 2019 to December 2023. Based on the information provided by the GLD360 dataset, we estimated that, over the Cerrado, the uncertainty on the location of a lightning strike - which we considered as the median length of the semi-major axis of the 95% confidence ellipse - was around 3.4 km (95% confidence interval, CI, (2.3, 7.8) km; Supplementary Figure 6 b). The uncertainty associated with the time of the lightning strike is on the order of milliseconds and, hence, negligible when compared to the temporal uncertainty of GFA ignition points. Further, the Global Lightning Detection Network may be missing some of the lightning strikes, which go undetected. However, a formal assessment of the uncertainty on the lightning detection efficiency is not available, nor an estimation of how the detection efficiency might vary spatially (as the location of the detectors is not disclosed). However, studies have shown that the GLD360 maps various number of magnitudes more lightning strikes than the Tropical Rainfall Monitoring Mission (TRMM) Lightning Imaging Sensor (LIS), and that the spatial patterns of lightning densities of both datasets are similar [82].

4.2.3 Ground truth data on lightning-caused fires

To assess the effectiveness of the fire cause attribution method, we used reference data on observations of fires caused by lightning recorded by the Instituto Chico Mendes de Conservação da Biodiversidade (ICMBio), which is responsible for managing, protecting, monitoring and inspecting the 340 Federal Conservation Units across Brazil. The data provided consisted of two types of datasets recording lightning fires observed in several protected areas across the Cerrado for the period 2020-2023: (a) a georeferenced dataset providing manually drawn polygons of lightning fires with the date of ignition (Supplementary Table 1), and (b) a non-georeferenced tabular dataset containing records on the detection of lightning fires (Supplementary Table 2). This non-georeferenced dataset (b) contained information on the

protected area where the fire occurred, the estimated date of ignition, and the type of management intervention (e.g. if the fire was suppressed or no action was taken). The tabular dataset (b) included all the fire events recorded in the georeferenced data (a), in addition to other lightning fire occurrences.

4.2.4 Land-use data

To quantify the level of landscape fragmentation across the Cerrado, and hence the level of agricultural presence, we used land use and land cover data from the MapBiomas project (Collection 8.0 [92]), which uses the random forest algorithm to classify annual mosaics of Landsat images (30 m spatial resolution). MapBiomas is an open source and open data project that uses Google Earth Engine [98] to develop their products.

We divided the Cerrado into a 30 km grid, and calculated for each grid cell and year the percentage area occupied by non-converted vegetation - as opposed to human land use area. We simplified MapBiomas Collection 8.0 land use and land cover classes into "anthropic" and "natural" groups, the first comprising "Urban Area", "Mining" and all subcategories under "Farming"; the second comprising all subcategories under "Forest", as well as "Wetland" and "Grassland". Hence, the percentage of natural area was calculated as the percentage of pixels classified as "natural" out of the union of "natural" and "anthropic". Because the MapBiomas Collection 8.0 [92] was the last available version at the time of the study and it went only up to the year 2022, we used the land use and land cover data from this year for all those fires in the year 2023.

4.2.5 Climate data

We used climate data to characterise the weather conditions in which the fires took place. We used daily precipitation data from the Climate Hazards Group InfraRed Precipitation with Station data (CHIRPS, version 2.0), a quasi-global rainfall dataset with 0.05° spatial resolution for the period 1981-present [99]. We used the CHIRPS data product for precipitation as it has been identified as the most reliable dataset for precipitation in tropical climates [100]. For each ignition point provided by the GFA, we calculated the accumulated precipitation over the 10 days prior to the ignition day (the start day of the fire as provided by the GFA).

We used the 2-metre temperature and 2-metre dewpoint temperature from the climate re-analysis dataset ERA5-Land Daily Aggregated product [101], with a 9 km resolution, to calculate the vapour pressure deficit (VPD) - the difference between saturation pressure (e_s) and actual vapour pressure (e_a) [102]. We calculated the VPD on the day of ignition. We used temperature data from ERA5-Land dataset because it is one of the most reliable data products for temperature for tropical climates [100].

4.2.6 Infrastructure data

We used data on two types of infrastructure, roads and urban areas (Supplementary Figure 7). We obtained the road data as georeferenced files from the MapBiomas project website [103], which in turn compiled this data from various sources, including the Geographic and Statistics Institute of Brazil (Instituto Brasileiro de Geografia e Estatística, IBGE). We used the MapBiomas Collection 8.0 [92] classifications to create georeferenced polygons of urban areas by drawing polygons of all "Urban Area" pixels for each year.

4.3 Data analysis

All data processing and analysis in this study were carried out using Python programming language and Jupyter Notebook [104].

4.3.1 Ignition cause attribution method

To identify fires most likely ignited by lightning, we searched for those GFA polygons that co-occurred in space and time with a lightning strike. However, because of the uncertainties in the spatial and temporal location of the fire events and lightning strikes of the datasets used, any attribution method had to allow a certain time lag and spatial gap between the time and location of the observed lightning strikes and those of the ignition points.

Here, we followed the method of Larjavaara et al. [55] that assigns an attribution score, B, to every fire quantifying how likely each one is to have been ignited by lightning [55], and which has been previously applied to the Pantanal wetland [27] in Brazil. Following this method, all lightning strikes within certain spatial and temporal windows are considered to be ignition candidates, but their contribution to the attribution score depends on how far in space and time they are from the ignition point.

This method is implemented in four steps. First, the temporal, Δt_{max}, and spatial, Δx_{max}, windows are selected. Then, every lightning strike, i, and fire, j, pair is assigned a proximity index, $A_{i,j}$, that weights their spatial and temporal separation,

$$A_{i,j} = \begin{cases} \left(1 - \dfrac{\Delta t_{i,j}}{\Delta t_{\text{max}}}\right)\left(1 - \dfrac{\Delta x_{i,j}}{\Delta x_{\text{max}}}\right) & \text{when } \Delta t_{i,j} < \Delta t_{\text{max}} \text{ and } \Delta x_{i,j} < \Delta x_{\text{max}}, \\ 0 & \text{otherwise.} \end{cases} \quad (1)$$

$\Delta t_{i,j}$ expresses the time lag and $\Delta x_{i,j}$ the spatial distance between the lightning strike and the ignition point. This proximity index ranges between 1 (perfect co-occurrence) and 0 (the lightning strike falls outside the temporal or the spatial windows).

Once the lightning strike candidates are identified and their proximity index quantified,

the attribution scores, B_j, for a fire j are calculated as

$$B_j = 1 - \prod_{i=1}^{n_j}(1 - A_{i,j}), \tag{2}$$

where n_j is the number of lightning candidates for fire j. Finally, all those fires with an attribution score larger than or equal to some threshold, B_{thresh}, are considered to be ignited by lightning.

Hence, this attribution method requires making a number of decisions concerning the values of Δt_{max}, Δx_{max}, and B_{thresh}. The choice of these values should aim to balance omission and commission errors.

4.3.2 Attribution score thresholds (B) and windows (Δt_{max} and Δx_{max})

Following Menezes et al. [27], we used a rather high attribution score threshold, $B_{\text{thresh}} = 0.8$, to identify the fires most likely caused by lightning. In this manner, once the temporal and spatial windows were chosen, only those fires with higher attribution scores would be identified as likely caused by lightning. We then carried out a preliminary sensitivity analysis (Supplementary Figure 8) to understand how the proportion of lightning fires varied with different temporal and spatial windows considering a wide range of values, $\Delta t_{\text{max}} \in [1, 10]$ days and $\Delta x_{\text{max}} \in [2, 25]$ km. Further, to diminish confusion when comparing lightning and human-caused fires, we imposed a second attribution score threshold to identify those fires most likely caused by humans. Using again a conservative score, only those fires with $B \leq 0.2$ were identified as caused by humans. Finally, fires with attribution scores between 0.2 and 0.8 were considered as not having a clear ignition cause.

Regarding the spatial and temporal windows, instead of selecting a unique value as has been done before [105, 106, 107, 108], we selected a set of plausible combinations, $\{(\Delta t_{\text{max}}, \Delta x_{\text{max}})$, $\Delta t_{\text{max}} \in [3, 7]$ days and $\Delta x_{\text{max}} \in [6, 12]$ km$\}$. For each $(\Delta t_{\text{max}}, \Delta x_{\text{max}})$ pair, we identified those fires with $B \geq 0.8$ as caused by lightning, those with $B \leq 0.2$ as caused by humans, and the remaining fires (B between 0.2 and 0.8) as having no clear ignition cause. For each pair $(\Delta t_{\text{max}}, \Delta x_{\text{max}})$, we quantified the number and percentage of fires per ignition category (lightning, humans, or not clear), as well as the corresponding percentage of total burned area. Next, we estimated the final percentages for each ignition category as the average values obtained from all temporal and spatial window pairs, $\{(\Delta t_{\text{max}}, \Delta x_{\text{max}})\}$. Finally, we assessed how these percentages varied when using different $(\Delta t_{\text{max}}, \Delta x_{\text{max}})$ values, which we expressed as a 95% CI around the mean using the bootstrapping algorithm [109].

The time elapsed between the lightning strike and the moment the fire is first detected by an observer or detection device is commonly referred to as holdover time [110]. In this case, the detection time corresponds to the day of ignition provided by the GFA dataset, so the holdover time depends on when the Terra and Aqua satellites overpass the fire, the presence of

clouds [110] (particularly in the Cerrado [111, 112]), when the spectral signal from the burn scar becomes detectable by the MODIS instrument, and uncertainties on the day of burn, derived from the MCD64A1 burned area algorithm [57] and from the GFA dataset (around 2 to 4 days [26]).

Considering these sources of uncertainty, most studies identifying lightning-caused fires use a Δt_{max} around 5 days [27]. In this study, we considered a range of values, $\Delta t_{\text{max}} \in [3, 7]$ days, since MODIS uncertainty on the day of burn is ± 1 day in 45% of the cases, and can reach up to 6 days for the Cerrado [97]. This means that the GFA dataset could be reporting ignition dates around one day or more earlier than the actual start of the fire. Therefore, when running the attribution algorithm, we included as candidates all lightning strikes falling from Δt_{max} days before the GFA day of ignition to one day after.

Regarding Δx_{max}, the mismatch between the lightning strike location and that of the ignition point depends on the uncertainty of these two locations, as well as spatial mismatches derived from delays in the detection of the fire. As indicated earlier, the uncertainty in the location of the lightning strike could go up to 8 km, and that of the GFA ignition point up to 2.2 km (Supplementary Figure 6). Therefore, we considered $\Delta x_{\text{max}} \in [6, 12]$ km to identify fire-igniting lightning candidates. Again, this range is also in accordance with other studies, which usually consider spatial windows around 8-10 km [105, 106, 107].

4.3.3 Validation of the attribution method with ground truth data

We used both the georeferenced dataset (with fire polygons) and the non-georeferenced dataset (in tabular format) provided by ICMBio containing observed lightning-caused fires as ground truth data for our attribution method. Even though the number of records in the ICMBio dataset on lightning fires was too small to allow a full statistical validation, we used the two datasets to verify whether the attribution method was able to identify any of the ground truth records as caused by lightning. Although we could not use the ground truth data to select Δt_{max} and Δx_{max} values that balanced commission and omission errors of identification, we at least have an indication of whether it was able to identify any lightning fires at all.

Regarding the georeferenced vector dataset, a total of 11 fire polygons were selected after inspection of the data (Supplementary Table 1). Out of these, we found that 6 events had been mapped by the GFA dataset (i.e. GFA polygons overlapping in time and space with the corresponding ICMBio ground truth records). Next, we evaluated whether any of these 6 fires were identified as caused by lightning by the attribution method. We found that 5 of these had an attribution score $B > 0.8$ for at least one of the $(\Delta t_{\text{max}}, \Delta x_{\text{max}})$ combinations considered. The remaining fire had a score B between 0.7 and 0.8 for $\Delta x_{\text{max}} = 12$ km and all Δt_{max} considered (Supplementary Figure 9).

Even though the non-georeferenced tabular dataset did not provide the exact location of

fires, it indicated that in specific protected areas of the Cerrado and on specific dates some lightning-caused fires had occurred. Hence, as a further check to the attribution method, we explored whether there were any fire polygons in the GFA dataset overlapping these protected areas within a period up to five days before and one day after the ignition date recorded in the tabular ICMBio data, and whether any of these records had $B \geq 0.8$. In the non-georeferenced tabular data, there were 20 records reporting lightning-caused fires in different protected areas and dates (Supplementary Table 2). The GFA dataset detected 14 fire polygons corresponding to 7 out of these 20 tabular records. Out of these 14 fire polygons, we identified 13 polygons as likely caused by lightning ($B \geq 0.8$) (Supplementary Figure 9). The remaining polygon had, again, an attribution score B between 0.7 and 0.8. We also noted that these 13 fire polygons included the 6 fire polygons contained in the ICMBio georeferenced data.

Therefore, the attribution method was able to identify all the lightning fires except one. Still, this ground truth data only contains information about fires in protected areas where fire occurrence is possibly more controlled than in other areas of the Cerrado. We might expect the attribution method to have larger confounding error between human and lightning ignitions in areas of the Cerrado with high densities of fires like in agricultural frontiers. It is also worth noting that a large number of lightning fires in the ground truth data did not appear in the GFA dataset of, possibly related to the fact that most lightning fires are small or occur together with clouds [49], which diminishes their identification by coarse-resolution data products such as MODIS [62].

4.3.4 Characterising patterns of lightning and human-caused fires

We used the identification of the most likely ignition cause of fires to quantify the relative contribution of lightning and humans to fire ignitions over the Cerrado in the period 2019-2023. Because coarse burned area products MCD64A1 and GFA only map fires larger than 0.21 km^2 and have high omission errors among small fires [58, 59], we also calculated the overall percentage of lightning fires as we gradually removed small fires from the total count to understand the contribution of small fires to the total proportion of lightning fires.

To explore differences in the seasonality of lightning and human-caused fires, we calculated the number and percentage of fires created by each ignition type in each month. Further, we complemented this seasonal analysis with the typical weather conditions in terms of the average monthly VPD and total precipitation, as well as with the average number of lightning strikes, the lightning ignition efficiency (in terms of the number of lightning of strikes conducive to fires in a certain month over the total number of lightning strikes in the month), and the average number of lightning strikes per unit area and per unit precipitation volume (obtained as the average of the number of lightning strikes in a certain month over the Cerrado divided by the total area of the Cerrado and by the total precipitation in the month).

To characterise the spatial distribution of lightning and human-caused fires across the

Cerrado, we obtained the number of fires in each ignition category (lightning, human or not clear) for each 30 km grid cell, year, and combination of spatial and temporal windows. Then, for each cell and year, we calculated the average number and percentage of fires in each ignition category out of all the $\{(\Delta t_{\text{max}}, \Delta x_{\text{max}})\}$ combinations, and the corresponding 95% CI using bootstrapping. Finally, for each cell, we calculated the average annual number of fires of each ignition category, along with the 95% CI of the mean. Even though we took into account that a number of fires had no clear ignition cause when calculating the percentages, we focused the spatial analysis only on the lightning and human-caused fires. Similarly, we explored the geographical patterns of lightning densities by counting the number of strikes per grid cell and year and calculating the annual average number of lightning densities. Again, we also calculated the 95% CI around the mean.

We quantified the fire frequencies of human ($B \leq 0.2$) and lightning-ignited ($B \geq 0.8$) fires. In this case, we used $\Delta t_{\text{max}} = 5$ days and $\Delta x_{\text{max}} = 9$ km, the middle values out of all temporal and spatial window combinations considered earlier, to identify the ignition causes of each GFA polygon. Then, to calculate the fire frequencies, we counted how many times each pixel had burned in the period for each ignition cause. Therefore, fire frequencies would range from 1 year to 5 consecutive years in the period 2019 to 2023. Finally, to compare the fire frequencies between lightning and human-caused fires, we normalised the pixel count (equivalent to burned area) of each frequency and ignition cause by the corresponding total number of affected pixels (the total area that burned at least once for that type of ignition).

To evaluate the influence of climate and landscape configuration, we compared the conditions in which the human-caused ($B \leq 0.2$) and the lightning-caused ($B \geq 0.8$) fires took place, both in terms of the weather and fuel conditions at ignition, and in terms of the level of fragmentation of the landscapes where the fires happened. We used precipitation accumulated over the ten days prior to the ignition of the fire, and VPD on the ignition day as proxies for fuel flammability. Both weather and fragmentation are known to affect fire behaviour [17]. Again, we used $\Delta t_{\text{max}} = 5$ days and $\Delta x_{\text{max}} = 9$ km to identify the most likely ignition causes of the fires.

We characterised the landscape in which each fire took place in terms of the percentage of natural area of the grid cell and year of ignition. We did the same for each lightning strike in the study period. We then classified the occurrences of each type of event (lightning-caused fires, human-caused fires and lightning strikes) according to the percentage of natural area - a proxy for the level of fragmentation. To understand how each type of event was distributed across landscapes with different proportions of natural area, we divided the number of occurrences in a decile by the total area occupied by that decile of natural area.

Further, for each GFA polygon, we also calculated the distance from the ignition point to the closest road and to the closest urban area. Because the distance distributions we obtained for lightning-caused fires were skewed towards small values for both types of infrastructure, we also calculated the shortest distances for all lightning strikes in the period. In this manner, we

could interpret whether the skewness of the distance distribution could be related to lightning strikes being more likely to fall close to these two types of infrastructure.

Finally, we compared the fire behaviour of lightning and human-caused fires focusing on fire size and median FRP. We also explored the distribution of these two variables per decile of natural area percentage because the level of landscape fragmentation can also affect fire behaviour using, again, $\Delta t_{\text{max}} = 5$ days and $\Delta x_{\text{max}} = 9$ km. Because of their disproportionate effects on ecosystems despite their typical low numbers, we furhter compared the largest (fire size ≥ 150 km^2) and the most intense (median FRP ≥ 100 MW) fires separately by ignition cause. For each of these two variables, we explored the weather conditions at ignition against the level of natural area percentage of the landscape where they took place.

Data availability statement

The climate data used in this study are publicly available from ERA5-Land Daily Averaged at `https://www.ecmwf.int/en/forecasts/dataset/ecmwf-reanalysis-v5-land`, and Climate Hazards Group InfraRed Precipitation with Station data version 2.0 at `https://data.chc.ucsb.edu/products/CHIRPS-2.0/`. The land use data are publicly available from MapBiomas collection 8.0 at `https://brasil.mapbiomas.org/en/colecoes-mapbiomas/`. The Global Fire Atlas data are publicly available from `https://zenodo.org/records/11400062`. The lightning strikes data from the Vaisala Global Lightning Detection Network GLD360 will soon be made publicly available [113] in a coarsened format as it is subject to contractual agreement. The processed data is available at `https://doi.org/10.5281/zenodo.19683855`.

Code availability statement

The code supporting this study is available at `https://doi.org/10.5281/zenodo.19683855`, together with the processed data. Custom code scripts were all written in Python 3.9, including scripts used to create figures. Some figures were further adjusted (placing of labels and text) using Inkscape v1.2.2. Supplementary Figure 7 was created using QGIS 3.34.6.

Competing interests

The authors declare no competing interests.

Acknowledgements

We thank Esther Brambleby for subsetting and formatting the lightning data. We thank the Ecosystems Lab Group at the Environmental Change Institute, School of Geography and the Environment, University of Oxford, for helpful feedback during discussions. We also thank the Instituto Chico Mendes de Conservação da Biodiversidade (ICMBio) for the ground truth data on lightning-ignited fires in Cerrado's protected areas.

Funding Statement

C.S.G. discloses support for the research of this work from the UK Natural Environment Research Council under grant number NE/S007474/1.

Author Contributions

C.S.G.: Conceptualization, Methodology, Software, Formal Analysis, Investigation, Data Curation, Writing - Original Draft, Visualization, Funding acquisition. T.A.J.J.: Conceptualization, Methodology, Writing - Review and Editing, Visualization. R.L., L.S.M., G.M: Conceptualization, Resources, Writing - Review and Editing. S.V., M.W.J: Conceptualization, Methodology, Resources, Writing - Review and Editing. I.O.M: Conceptualization, Methodology, Resources, Writing - Review and Editing, Supervision, Project administration.

References

[1] William J. Bond. "Fires in the Cenozoic: a late flowering of flammable ecosystems". In: *Frontiers in Plant Science* 5 (2015). DOI: 10.3389/fpls.2014.00749.

[2] W Bond and J Keeley. "Fire as a global 'herbivore': the ecology and evolution of flammable ecosystems". In: *Trends in Ecology & Evolution* 20.7 (2005), pp. 387–394. DOI: 10.1016/j.tree.2005.04.025.

[3] Juli G. Pausas and Jon E. Keeley. "A Burning Story: The Role of Fire in the History of Life". In: *BioScience* 59.7 (2009), pp. 593–601. DOI: 10.1525/bio.2009.59.7.10.

[4] David J. Beerling and Colin P. Osborne. "The origin of the savanna biome". In: *Global Change Biology* 12.11 (2006), pp. 2023–2031. DOI: 10.1111/j.1365-2486.2006.01239.x.

[5] William A. Hoffmann, Birgit Orthen, and Paula Kielse Vargas do Nascimento. "Comparative fire ecology of tropical savanna and forest trees: *Fire traits of savanna and forest trees*". In: *Functional Ecology* 17.6 (2003), pp. 720–726. DOI: 10.1111/j.1365-2435.2003.00796.x.

[6] Marcelo F. Simon and Toby Pennington. "Evidence for Adaptation to Fire Regimes in the Tropical Savannas of the Brazilian Cerrado". In: *International Journal of Plant Sciences* 173.6 (2012), pp. 711–723. DOI: 10.1086/665973.

[7] Juli G. Pausas, Jon E. Keeley, and Dylan W. Schwilk. "Flammability as an ecological and evolutionary driver". In: *Journal of Ecology* 105.2 (2017). Ed. by Mark Rees, pp. 289–297. DOI: 10.1111/1365-2745.12691.

[8] Tianhua He et al. "Fire-adapted traits of Pinus arose in the fiery Cretaceous". In: *New Phytologist* 194.3 (2012), pp. 751–759. DOI: 10.1111/j.1469-8137.2012.04079.x.

[9] Tianhua He, Byron B Lamont, and John Manning. "A Cretaceous origin for fire adaptations in the Cape flora". In: *Scientific Reports* 6.34880 (2016). DOI: 10.1038/srep34880.

[10] I.J. Glasspool, D. Edwards, and L. Axe. "Charcoal in the Silurian as evidence for the earliest wildfire". In: *Geology* 32.5 (2004), p. 381. DOI: 10.1130/G20363.1.

[11] Immaculada Oliveras and Yadvinder Malhi. "Many shades of green: the dynamic tropical forest–savannah transition zones". In: *Philosophical Transactions of the Royal Society B: Biological Sciences* 371.1703 (2016), p. 20150308. DOI: 10.1098/rstb.2015.0308.

[12] Juli G. Pausas and William J. Bond. "Alternative Biome States in Terrestrial Ecosystems". In: *Trends in Plant Science* 25.3 (2020), pp. 250–263. DOI: 10.1016/j.tplants.2019.11.003.

[13] Sally Archibald, A. Carla Staver, and Simon A. Levin. "Evolution of human-driven fire regimes in Africa". In: *Proceedings of the National Academy of Sciences* 109.3 (2012), pp. 847–852. DOI: 10.1073/pnas.1118648109.

[14] Jos Barlow et al. "Clarifying Amazonia's burning crisis". In: *Global Change Biology* 26.2 (2020), pp. 319–321. DOI: 10.1111/gcb.14872.

[15] David M. J. S. Bowman et al. "Fire in the Earth System". In: *Science* 324.5926 (2009), pp. 481–484. DOI: 10.1126/science.1163886.

[16] S Archibald et al. "Biological and geophysical feedbacks with fire in the Earth system". In: *Environmental Research Letters* 13.3 (2018), p. 033003. DOI: 10.1088/1748-9326/aa9ead.

[17] Sally Archibald et al. "What limits fire? An examination of drivers of burnt area in Southern Africa". In: *Global Change Biology* 15.3 (2009), pp. 613–630. DOI: 10.1111/j.1365-2486.2008.01754.x.

[18] Jennifer K. Balch et al. "Human-started wildfires expand the fire niche across the United States". In: *Proceedings of the National Academy of Sciences* 114.11 (2017), pp. 2946–2951. DOI: 10.1073/pnas.1617394114.

[19] Stijn Hantson et al. "Human-ignited fires result in more extreme fire behavior and ecosystem impacts". In: *Nature Communications* 13.1 (2022), p. 2717. DOI: 10.1038/s41467-022-30030-2.

[20] Stefan H. Doerr and Cristina Santín. "Global trends in wildfire and its impacts: perceptions versus realities in a changing world". In: *Philosophical Transactions of the Royal Society B: Biological Sciences* 371.1696 (2016), p. 20150345. DOI: 10.1098/rstb.2015.0345.

[21] Megan E Cattau et al. "Anthropogenic and lightning-started fires are becoming larger and more frequent over a longer season length in the USA". In: *Global Ecology and Biogeography* 29.4 (2020), pp. 668–681. DOI: 10.1111/geb.13058.

[22] W. Matt Jolly et al. "Climate-induced variations in global wildfire danger from 1979 to 2013". In: *Nature Communications* 6.1 (2015), p. 7537. DOI: 10.1038/ncomms8537.

[23] Sander Veraverbeke et al. "Lightning as a major driver of recent large fire years in North American boreal forests". In: *Nature Climate Change* 7.7 (2017), pp. 529–534. DOI: 10.1038/nclimate3329.

[24] Hugh J. Christian et al. "Global frequency and distribution of lightning as observed from space by the Optical Transient Detector". In: *Journal of Geophysical Research: Atmospheres* 108 (D1 2003). DOI: 10.1029/2002JD002347.

[25] Thomas A. J. Janssen et al. "Extratropical forests increasingly at risk due to lightning fires". In: *Nature Geoscience* 16 (2023), pp. 1136–1144. DOI: 10.1038/s41561-023-01322-z.

[26] Niels Andela et al. "The Global Fire Atlas of individual fire size, duration, speed and direction". In: *Earth System Science Data* 11 (2019), pp. 529–552. DOI: 10.5194/essd-11-529-2019.

[27] Lucas S Menezes. "Lightning patterns in the Pantanal: Untangling natural and anthropogenic-induced wildfires". In: *Science of the Total Environment* 820 (2022), p. 153021. DOI: 10.1016/j.scitotenv.2022.153021.

[28] Eduardo Da Silva Pinheiro and Giselda Durigan. "Dinâmica espaço-temporal (1962-2006) das fitofisionomias em unidade de conservação do Cerrado no sudeste do Brasil". In: *Revista Brasileira de Botânica* 32.3 (2009), pp. 441–454. DOI: 10.1590/S0100-84042009000300005.

[29] J. A. Ratter, S. Bridgewater, and J. F. Ribeiro. "Analysis of the floristic composition of the Brazilian Cerrado vegetation III: comparison of the woody vegetation of 376 areas". In: *Edinburgh Journal of Botany* 60.1 (2003), pp. 57–109. DOI: 10.1017/S0960428603000064.

[30] J.F. Ribeiro and B.M.T. Walter. "Cerrado Ecologia e Flora". In: *As principais fitofisionomias do Bioma Cerrado*. Embrapa, 2008, pp. 152–212.

[31] Marcelo F. Simon et al. "Recent assembly of the Cerrado, a neotropical plant diversity hotspot, by in situ evolution of adaptations to fire". In: *Proceedings of the National Academy of Sciences* 106.48 (2009), pp. 20359–20364. DOI: 10.1073/pnas.0903410106.

[32] George Eiten. "The cerrado vegetation of Brazil". In: *The Botanical Review* 38.2 (1972), pp. 201–341. DOI: 10.1007/BF02859158.

[33] L. M. Coutinho. "Ecological Effects of Fire in Brazilian Cerrado". In: *Ecology of Tropical Savannas*. Ed. by Brian J. Huntley and Brian H. Walker. Red. by W. D. Billings et al. Vol. 42. Series Title: Ecological Studies. Berlin, Heidelberg: Springer Berlin Heidelberg, 1982, pp. 273–291. DOI: 10.1007/978-3-642-68786-0_13.

[34] Jayalaxshmi Mistry, Bibiana A. Bilbao, and Andrea Berardi. "Community owned solutions for fire management in tropical ecosystems: case studies from Indigenous communities of South America". In: *Philosophical Transactions of the Royal Society B: Biological Sciences* 371.1696 (2016), p. 20150174. DOI: 10.1098/rstb.2015.0174.

[35] Jayalaxshmi Mistry et al. "New perspectives in fire management in South American savannas: The importance of intercultural governance". In: *Ambio* 48.2 (2019), pp. 172–179. DOI: 10.1007/s13280-018-1054-7.

[36] Jayalaxshmi Mistry et al. "Indigenous Fire Management in the cerrado of Brazil: The Case of the Krahô of Tocantíns". In: *Human Ecology* 33.3 (2005), pp. 365–386. DOI: 10.1007/s10745-005-4143-8.

[37] James R. Welch et al. "Indigenous Burning as Conservation Practice: Neotropical Savanna Recovery amid Agribusiness Deforestation in Central Brazil". In: *PLoS ONE* 8.12 (2013). Ed. by Brock Fenton, e81226. DOI: 10.1371/journal.pone.0081226.

[38] Ludivine Eloy et al. "Seasonal fire management by traditional cattle ranchers prevents the spread of wildfire in the Brazilian Cerrado". In: *Ambio* 48.8 (2019), pp. 890–899. DOI: 10.1007/s13280-018-1118-8.

[39] Giselda Durigan et al. "No Net Loss of Species Diversity After Prescribed Fires in the Brazilian Savanna". In: *Frontiers in Forests and Global Change* 3 (2020), p. 13. DOI: 10.3389/ffgc.2020.00013.

[40] Alessandra Fidelis et al. "The Year 2017: Megafires and Management in the Cerrado". In: *Fire* 1.3 (2018), p. 49. DOI: 10.3390/fire1030049.

[41] Mônica Martins Melo and Carlos Hiroo Saito. "Regime de queima das caçadas com uso do fogo realizadas pelos Xavante no Cerrado". In: *Biodiversidade Brasileira* 1.2 (2011), pp. 97–109. DOI: 10.37002/biodiversidadebrasileira.v1i2.110.

[42] Lea Rekow. "Socio-Ecological Implications of Soy in the Brazilian Cerrado". In: *Challenges in Sustainability* 7.1 (2019), pp. 7–29. DOI: 10.12924/cis2019.07010007.

[43] Ane Alencar et al. "Mapping Three Decades of Changes in the Brazilian Savanna Native Vegetation Using Landsat Data Processed in the Google Earth Engine Platform". In: *Remote Sensing* 12.6 (2020), p. 924. DOI: 10.3390/rs12060924.

[44] Patrícia S. Silva et al. "Putting fire on the map of Brazilian savanna ecoregions". In: *Journal of Environmental Management* 296 (2021), p. 113098. DOI: 10.1016/j.jenvman.2021.113098.

[45] Carlota Segura-Garcia et al. "Human land occupation regulates the effect of the climate on the burned area of the Brazilian Cerrado". In: *Communications Earth & Environment* 5.1 (2024), p. 361. DOI: 10.1038/s43247-024-01521-5.

[46] Vera Laísa da Silva Arruda et al. "Assessing four decades of fire behavior dynamics in the Cerrado biome (1985 to 2022)". In: *Fire Ecology* 20.1 (2024), p. 64. DOI: 10.1186/s42408-024-00298-4.

[47] Dhemerson E. Conciani et al. "Human-climate interactions shape fire regimes in the Cerrado of São Paulo state, Brazil". In: *Journal for Nature Conservation* 61 (2021), p. 126006. DOI: 10.1016/j.jnc.2021.126006.

[48] Vânia R. Pivello. "The Use of Fire in the Cerrado and Amazonian Rainforests of Brazil: Past and Present". In: *Fire Ecology* 7.1 (2011), pp. 24–39. DOI: 10.4996/fireecology.0701024.

[49] Vanúcia Schumacher et al. "Characteristics of lightning-caused wildfires in central Brazil in relation to cloud-ground and dry lightning". In: *Agricultural and Forest Meteorology* 312 (2022), p. 108723. DOI: 10.1016/j.agrformet.2021.108723.

[50] Guilherme Augusto Verola Mataveli et al. *Analysis of fire dynamics in the Brazilian savannas*. preprint. Other Hazards (e.g., Glacial, Snow Hazards, Karst, Wildfires Hazards, and Medical Geo-Hazards), 2017. DOI: 10.5194/nhess-2017-90.

[51] Mário Barroso Ramos-Neto and Vânia Regina Pivello. "Lightning Fires in a Brazilian Savanna National Park: Rethinking Management Strategies". In: *Environmental Management* 26.6 (2000), pp. 675–684. DOI: 10.1007/s002670010124.

[52] Alfredo Pereira and Helena França. "Identificação de queimadas naturais ocorridas no período chuvoso de 2003-2004 no Parque Nacional das Emas, Brasil, por meio de imagens dos sensores do satélite CBERS-2". In: *Anais XII Simpósio Brasileiro de Sensoriamento Remoto, Goiânia, Brasil, INPE* (2005), pp. 3245–3252.

[53] Marcelo Brilhante de Medeiros and Nilton Cezar Fiedler. "Incêndios florestais no parque nacional da Serra da Canastra: desafios para a conservação da biodiversidade." In: *Ciência Florestal* 14.2 (2004), pp. 157–168. DOI: 10.5902/198050981815.

[54] Niels Andela and Matthew William Jones. *Update of: The Global Fire Atlas of individual fire size, duration, speed and direction*. Version v20240409. Zenodo, 2024. DOI: 10.5281/zenodo.11400062.

[55] M. Larjavaara, J. Pennanen, and T.J. Tuomi. "Lightning that ignites forest fires in Finland". In: *Agricultural and Forest Meteorology* 132.3 (2005), pp. 171–180. DOI: 10.1016/j.agrformet.2005.07.005.

[56] Nilton César Fiedler, Daniela Araújo Merlo, and Marcelo Brilhante de Medeiros. "Ocorrência de incêndios florestais no Parque Nacional da Chapada dos Veadeiros, Goiás." In: *Ciência Florestal* 16.2 (2006), pp. 153–161. DOI: 10.5902/198050981896.

[57] Louis Giglio, Wilfrid Schroeder, and Christopher O. Justice. "The collection 6 MODIS active fire detection algorithm and fire products". In: *Remote Sensing of Environment* 178 (2016), pp. 31–41. DOI: 10.1016/j.rse.2016.02.054.

[58] M.L. Campagnolo et al. "A comprehensive characterization of MODIS daily burned area mapping accuracy across fire sizes in tropical savannas". In: *Remote Sensing of Environment* 252 (2021), p. 112115. DOI: 10.1016/j.rse.2020.112115.

[59] Ruben Ramo et al. "African burned area and fire carbon emissions are strongly impacted by small fires undetected by coarse resolution satellite data". In: *Proceedings of the National Academy of Sciences* 118.9 (2021), e2011160118. DOI: 10.1073/pnas.2011160118.

[60] Edson E. Sano et al. "Cerrado ecoregions: A spatial framework to assess and prioritize Brazilian savanna environmental diversity for conservation". In: *Journal of Environmental Management* 232 (2019), pp. 818–828. DOI: 10.1016/j.jenvman.2018.11.108.

[61] Carlota Segura-Garcia et al. "The fire regimes of the Cerrado and their changes through time". In: *Philosophical Transactions B* 380.1924 (2025), p. 20230460. DOI: 10.1098/rstb.2023.0460.

[62] Julia A. Rodrigues et al. "How well do global burned area products represent fire patterns in the Brazilian Savannas biome? An accuracy assessment of the MCD64 collections". In: *International Journal of Applied Earth Observation and Geoinformation* 78 (2019), pp. 318–331. DOI: 10.1016/j.jag.2019.02.010.

[63] Hudson GV Fontenele and Heloisa S Miranda. "What happens when fire is too early? Observations of fire-stimulated fruit opening releasing underdeveloped seeds for an endemic Cerrado shrub". In: *Austral Ecology* 48.8 (2023), pp. 2246–2252. DOI: 10.1111/aec.13436.

[64] Juli G Pausas and Jon E Keeley. "Wildfires and global change". In: *Frontiers in Ecology and the Environment* 19.7 (2021), pp. 387–395. DOI: 10.1002/fee.2359.

[65] Laís Fernandes de Souza Neves et al. "Dinâmica do fogo no Parque Estadual do Araguaia, zona de transição Amazônia-Cerrado". In: *Ra'e Ga* 44 (2018), pp. 85–103. DOI: 10.5380/raega.

[66] Vagner Zanzarini, Alan N. Andersen, and Alessandra Fidelis. "Flammability in tropical savannas: Variation among growth forms and seasons in Cerrado". In: *Biotropica* 54.4 (2022), pp. 979–987. DOI: 10.1111/btp.13121.

[67] Thomas D Hessilt et al. "Future increases in lightning ignition efficiency and wildfire occurrence expected from drier fuels in boreal forest ecosystems of western North America". In: *Environ. Res. Lett.* 17.5 (2022), p. 054008. DOI: 10.1088/1748-9326/ac6311.

[68] Victor Hugo Rohden Prudente et al. "Limitations of cloud cover for optical remote sensing of agricultural areas across South America". In: *Remote Sensing Applications: Society and Environment* 20 (2020), p. 100414. DOI: 10.1016/j.rsase.2020.100414.

[69] Guilherme Augusto Verola Mataveli et al. "Satellite observations for describing fire patterns and climate-related fire drivers in the Brazilian savannas". In: *Natural Hazards and Earth System Sciences* 18.1 (2018), pp. 125–144. DOI: 10.5194/nhess-18-125-2018.

[70] Vânia R. Pivello et al. "Understanding Brazil's catastrophic fires: Causes, consequences and policy needed to prevent future tragedies". In: *Perspectives in Ecology and Conservation* 19.3 (2021), pp. 233–255. DOI: 10.1016/j.pecon.2021.06.005.

[71] A Carla Staver, Sally Archibald, and Simon A Levin. "The global extent and determinants of savanna and forest as alternative biome states". In: *Science* 334.6053 (2011), pp. 230–232. DOI: 10.1126/science.1210465.

[72] Marina Hirota et al. "Global resilience of tropical forest and savanna to critical transitions". In: *Science* 334.6053 (2011), pp. 232–235. DOI: 10.1126/science.121065.

[73] MB Medeiros and HS Miranda. "Post-fire resprouting and mortality in cerrado woody plant species over a three-year period". In: *Edinburgh Journal of Botany* 65.1 (2008), pp. 53–68. DOI: 10.1017/S0960428608004708.

[74] Giselda Durigan and James A Ratter. "The need for a consistent fire policy for Cerrado conservation". In: *Journal of Applied Ecology* 53.1 (2016), pp. 11–15. DOI: 10.1111/1365-2664.12559.

[75] Thais M Rosan et al. "Extensive 21st-century woody encroachment in South America's savanna". In: *Geophysical Research Letters* 46.12 (2019), pp. 6594–6603. DOI: 10.1029/2019GL082327.

[76] Allan Spessa, Bevan McBeth, and Colin Prentice. "Relationships among fire frequency, rainfall and vegetation patterns in the wet–dry tropics of northern Australia: an analysis based on NOAA-AVHRR data". In: *Global Ecology and Biogeography* 14.5 (2005), pp. 439–454. DOI: 10.1111/j.1466-822x.2005.00174.x.

[77] Jeremy Russell-Smith et al. "Bushfires 'down under': patterns and implications of contemporary Australian landscape burning". In: *International Journal of Wildland Fire* 16.4 (2007), p. 361. DOI: 10.1071/WF07018.

[78] Fabio Teixeira Pitta and Gerardo Cerdas Vega. "Impacts of the agribusiness expansion in the Matopiba region: communities and the environment". In: *ActionAid - Rio de Janeiro* (2017).

[79] P S Silva et al. "Drivers of burned area patterns in Cerrado: the case of MATOPIBA region". In: (2020), pp. 542–547.

[80] Andreia F. S. Ribeiro et al. "The time since land-use transition drives changes in fire activity in the Amazon-Cerrado region". In: *Communications Earth & Environment* 5.1 (2024), p. 96. DOI: 10.1038/s43247-024-01248-3.

[81] Gian Luca Spadoni et al. "Devegetation is a widespread driver of fire in the Brazilian Cerrado". In: *Journal of Environmental Management* 385 (2025), p. 125637. DOI: 0.1016/j.jenvman.2025.125637.

[82] Scott D Rudlosky, Michael J Peterson, and Douglas T Kahn. "GLD360 performance relative to TRMM LIS". In: *Journal of Atmospheric and Oceanic Technology* 34.6 (2017), pp. 1307–1322. DOI: 10.1175/JTECH-D-16-0243.1.

[83] R. Libonati et al. "Twenty-first century droughts have not increasingly exacerbated fire season severity in the Brazilian Amazon". In: *Scientific Reports* 11.1 (2021), p. 4400. DOI: 10.1038/s41598-021-82158-8.

[84] Stijn Hantson, Salvador Pueyo, and Emilio Chuvieco. "Global fire size distribution is driven by human impact and climate". In: *Global Ecology and Biogeography* 24.1 (2015). Publisher: Wiley Online Library, pp. 77–86. DOI: 10.1111/geb.12246.

[85] Olivia Haas, Iain Colin Prentice, and Sandy P Harrison. "Global environmental controls on wildfire burnt area, size, and intensity". In: *Environmental Research Letters* 17.6 (2022), p. 065004. DOI: 10.1088/1748-9326/ac6a69.

[86] Heloisa S Miranda, Mercedes MC Bustamante, and Antonio C Miranda. "The fire factor". In: *The cerrados of Brazil: ecology and natural history of a neotropical savanna*. Columbia University Press, 2002, pp. 51–68.

[87] Sally Archibald. "Managing the human component of fire regimes: lessons from Africa". In: *Philosophical Transactions of the Royal Society B: Biological Sciences* 371.1696 (2016), p. 20150346. DOI: 10.1098/rstb.2015.0346.

[88] Stephen J. Pyne. *Fire: A Brief History*. 2nd ed. University of Washington Press, 2019.

[89] Filippe L.M. Santos et al. "Prescribed Burning Reduces Large, High-Intensity Wildfires and Emissions in the Brazilian Savanna". In: *Fire* 4.3 (2021), p. 56. DOI: 10.3390/fire4030056.

[90] Ananda Santa Rosa de Andrade et al. "Implementation of Fire Policies in Brazil: An Assessment of Fire Dynamics in Brazilian Savanna". In: *Sustainability* 13.20 (2021), p. 11532. DOI: 10.3390/su132011532.

[91] Marcelo Brilhante de Medeiros. "Manejo do fogo em unidades de conservação do cerrado". In: *Boletim do Herbário Ezechias Paulo Heringer* 10 (2002).

[92] Carlos M. Souza et al. "Reconstructing Three Decades of Land Use and Land Cover Changes in Brazilian Biomes with Landsat Archive and Earth Engine". In: *Remote Sensing* 12.17 (2020), p. 2735. DOI: 10.3390/rs12172735.

[93] Carlos A. Klink and Ricardo B. Machado. "Conservation of the Brazilian Cerrado". In: *Conservation Biology* 19.3 (2005), pp. 707–713. DOI: 10.1111/j.1523-1739.2005.00702.x.

[94] Diego Tarley Ferreira Nascimento and Giuliano Tostes Novais. "Clima do Cerrado: dinâmica atmosférica e características, variabilidades e tipologias climáticas". In: *Élisée-Revista de Geografia da UEG* 9.2 (2020), e922021–e922021.

[95] Norman Myers et al. "Biodiversity hotspots for conservation priorities". In: *Nature* 403.6772 (2000), pp. 853–858. DOI: 10.1038/35002501.

[96] Wilfrid Schroeder et al. "The New VIIRS 375 m active fire detection data product: Algorithm description and initial assessment". In: *Remote Sensing of Environment* 143 (2014). Publisher: Elsevier, pp. 85–96. DOI: 10.1016/j.rse.2013.12.008.

[97] Miguel M. Pinto et al. "A deep learning approach for mapping and dating burned areas using temporal sequences of satellite images". In: *ISPRS Journal of Photogrammetry and Remote Sensing* 160 (2020), pp. 260–274. DOI: 10.1016/j.isprsjprs.2019.12.014.

[98] Noel Gorelick et al. "Google Earth Engine: Planetary-scale geospatial analysis for everyone". In: *Remote sensing of Environment* 202 (2017). Publisher: Elsevier, pp. 18–27. DOI: 10.1016/j.rse.2017.06.031.

[99] Chris Funk et al. "The climate hazards infrared precipitation with stations—a new environmental record for monitoring extremes". In: *Scientific Data* 2.1 (2015), p. 150066. DOI: 10.1038/sdata.2015.66.

[100] C. Burton, S. Rifai, and Y. Malhi. "Inter-comparison and assessment of gridded climate products over tropical forests during the 2015/2016 El Niño". In: *Philosophical Transactions of the Royal Society B: Biological Sciences* 373.1760 (2018), p. 20170406. DOI: 10.1098/rstb.2017.0406.

[101] Joaquín Muñoz-Sabater et al. "ERA5-Land: a state-of-the-art global reanalysis dataset for land applications". In: *Earth System Science Data* 13.9 (2021), pp. 4349–4383. DOI: 10.5194/essd-13-4349-2021.

[102] Richard G. Allen et al. *Crop evapotranspiration - Guidelines for computing crop water requirements*. FAO - Food and Agriculture Organization of the United Nations, 1998.

[103] MapBiomas Project. *Infrastructure, roads and urban areas data*. URL: https://brasil.mapbiomas.org/dados-de-infraestrutura/.

[104] Thomas Kluyver et al. "Jupyter Notebooks – a publishing format for reproducible computational workflows". In: *Positioning and Power in Academic Publishing: Players, Agents and Agendas*. Ed. by F. Loizides and B. Schmidt. IOS Press, 2016, pp. 87–90.

[105] Annalie Dorph et al. "Modelling ignition probability for human- and lightning-caused wildfires in Victoria, Australia". In: *Natural Hazards and Earth System Sciences* 22.10 (2022), pp. 3487–3499. DOI: 10.5194/nhess-22-3487-2022.

[106] Jose V. Moris et al. "Lightning-caused fires in the Alps: Identifying the igniting strokes". In: *Agricultural and Forest Meteorology* 290 (2020), p. 107990. DOI: 10.1016/j.agrformet.2020.107990.

[107] Francisco J. Pérez-Invernón et al. "Lightning-ignited wildfires and long continuing current lightning in the Mediterranean Basin: preferential meteorological conditions". In: *Atmospheric Chemistry and Physics* 21.23 (2021), pp. 17529–17557. DOI: 10.5194/acp-21-17529-2021.

[108] Francisco J. Pérez-Invernón, Heidi Huntrieser, and Jose V. Moris. "Meteorological Conditions Associated with Lightning Ignited Fires and Long-Continuing-Current Lightning in Arizona, New Mexico and Florida". In: *Fire* 5.4 (2022), p. 96. DOI: 10.3390/fire5040096.

[109] Siti Fairus Mokhtar, Zahayu Md Yusof, and Hasimah Sapiri. "Confidence intervals by bootstrapping approach: a significance review". In: *Malaysian Journal of Fundamental and Applied Sciences* 19.1 (2023), pp. 30–42.

[110] Jose V. Moris et al. "A global database on holdover time of lightning-ignited wildfires". In: *Earth System Science Data* 15.3 (2023), pp. 1151–1163. DOI: 10.5194/essd-15-1151-2023.

[111] Allan Pereira et al. "Burned Area Mapping in the Brazilian Savanna Using a One-Class Support Vector Machine Trained by Active Fires". In: *Remote Sensing* 9.11 (2017), p. 1161. DOI: 10.3390/rs9111161.

[112] Renata Libonati et al. "An Algorithm for Burned Area Detection in the Brazilian Cerrado Using 4 μm MODIS Imagery". In: *Remote Sensing* 7.11 (2015), pp. 15782–15803. DOI: 10.3390/rs71115782.

[113] Yuquan Qu et al. "FLASHMAP: A new global gridded lightning dataset with high spatial and temporal resolution". In: *EGU General Assembly 2026, Vienna, Austria, 3-8 May 2026* EGU26-532 (2026). DOI: 10.5194/egusphere-egu26-5328.

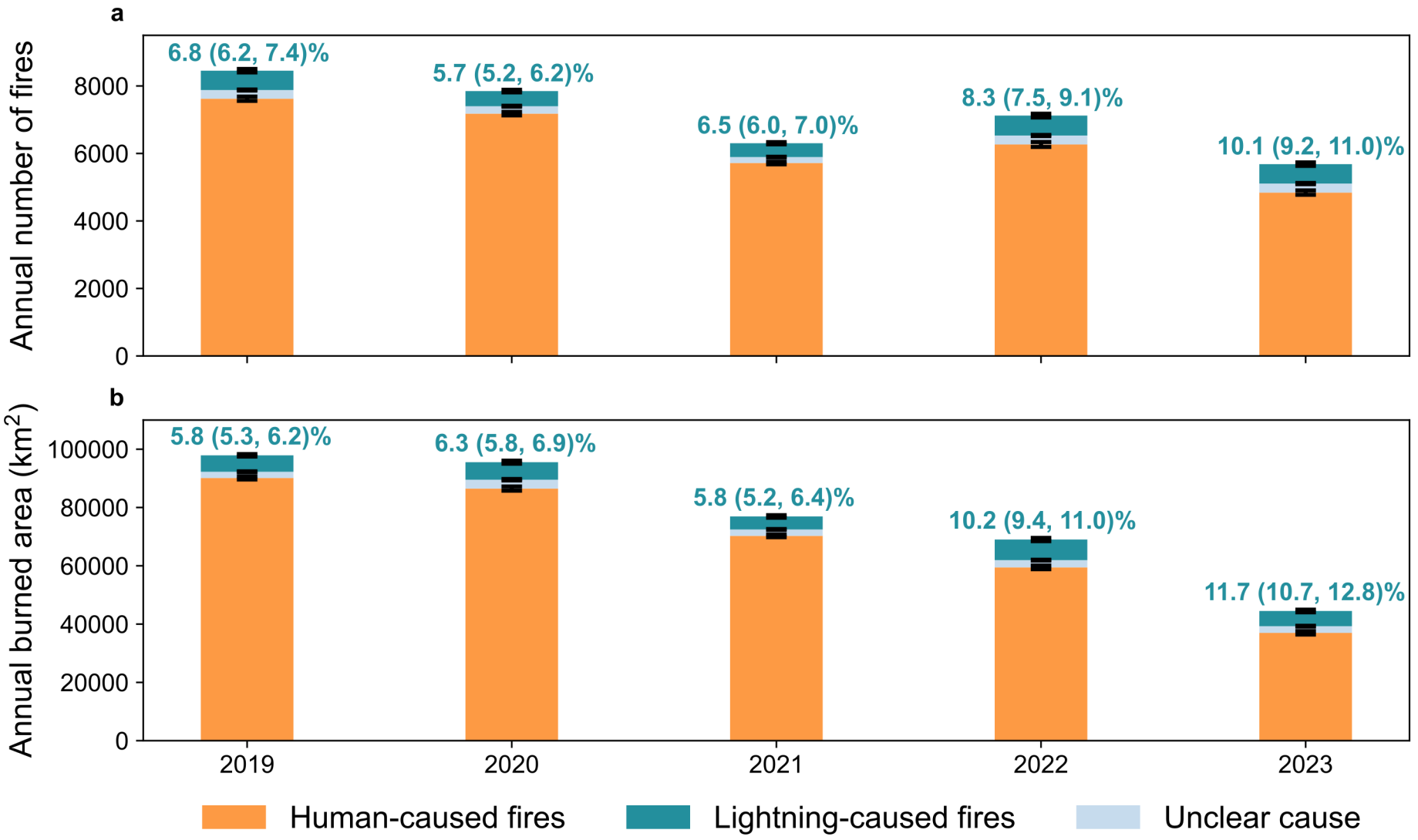
a
Annual number of fires
0
2000
4000
6000
8000
6.8 (6.2, 7.4)%
5.7 (5.2, 6.2)%
6.5 (6.0, 7.0)%
8.3 (7.5, 9.1)%
10.1 (9.2, 11.0)%
b
Annual burned area (km2)
0
20000
40000
60000
80000
100000
5.8 (5.3, 6.2)%
6.3 (5.8, 6.9)%
5.8 (5.2, 6.4)%
10.2 (9.4, 11.0)%
11.7 (10.7, 12.8)%
2019
2020
2021
2022
2023
Human-caused fires
Lightning-caused fires
Unclear cause

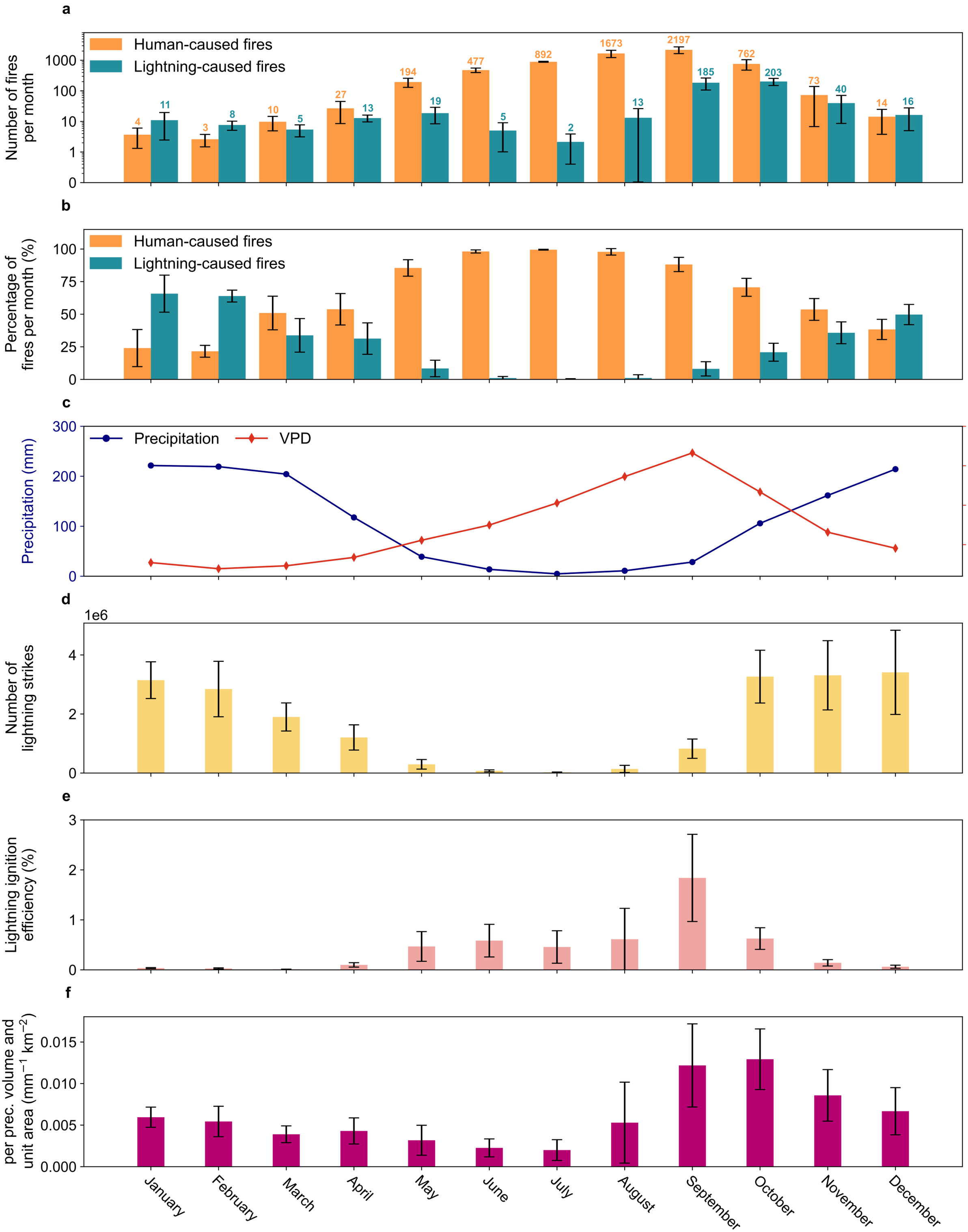
a
Human-caused fires
Lightning-caused fires
Number of fires per month
0
1
10
100
1000
4
11
3
8
10
5
27
13
194
19
477
5
892
2
1673
13
2197
185
762
203
73
40
14
16
b
Human-caused fires
Lightning-caused fires
Percentage of fires per month (%)
0
25
50
75
100
c
Precipitation
VPD
Precipitation (mm)
0
100
200
300
VPD (hPa)
10
15
20
25
d
1e6
Number of lightning strikes
0
2
4
e
Lightning ignition efficiency (%)
0
1
2
3
f
Lightning strikes per prec. volume and unit area (mm^{-1} km^{-2})
0.000
0.005
0.010
0.015
January
February
March
April
May
June
July
August
September
October
November
December

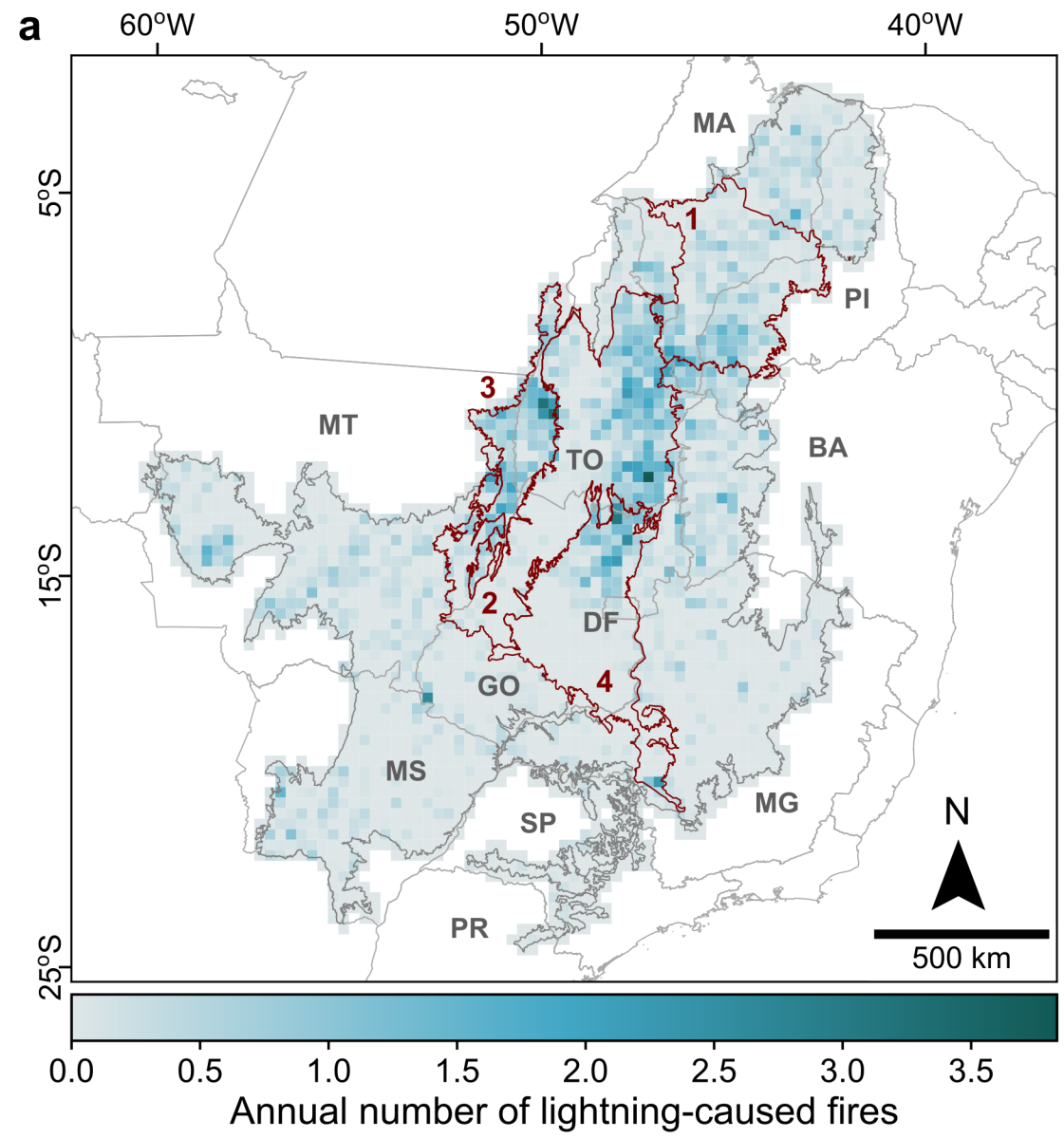
a
60°W
50°W
40°W
5°S
15°S
25°S
MA
PI
MT
BA
TO
DF
GO
MS
SP
MG
PR
1
2
3
4
N
500 km
0.0
0.5
1.0
1.5
2.0
2.5
3.0
3.5
Annual number of lightning-caused fires

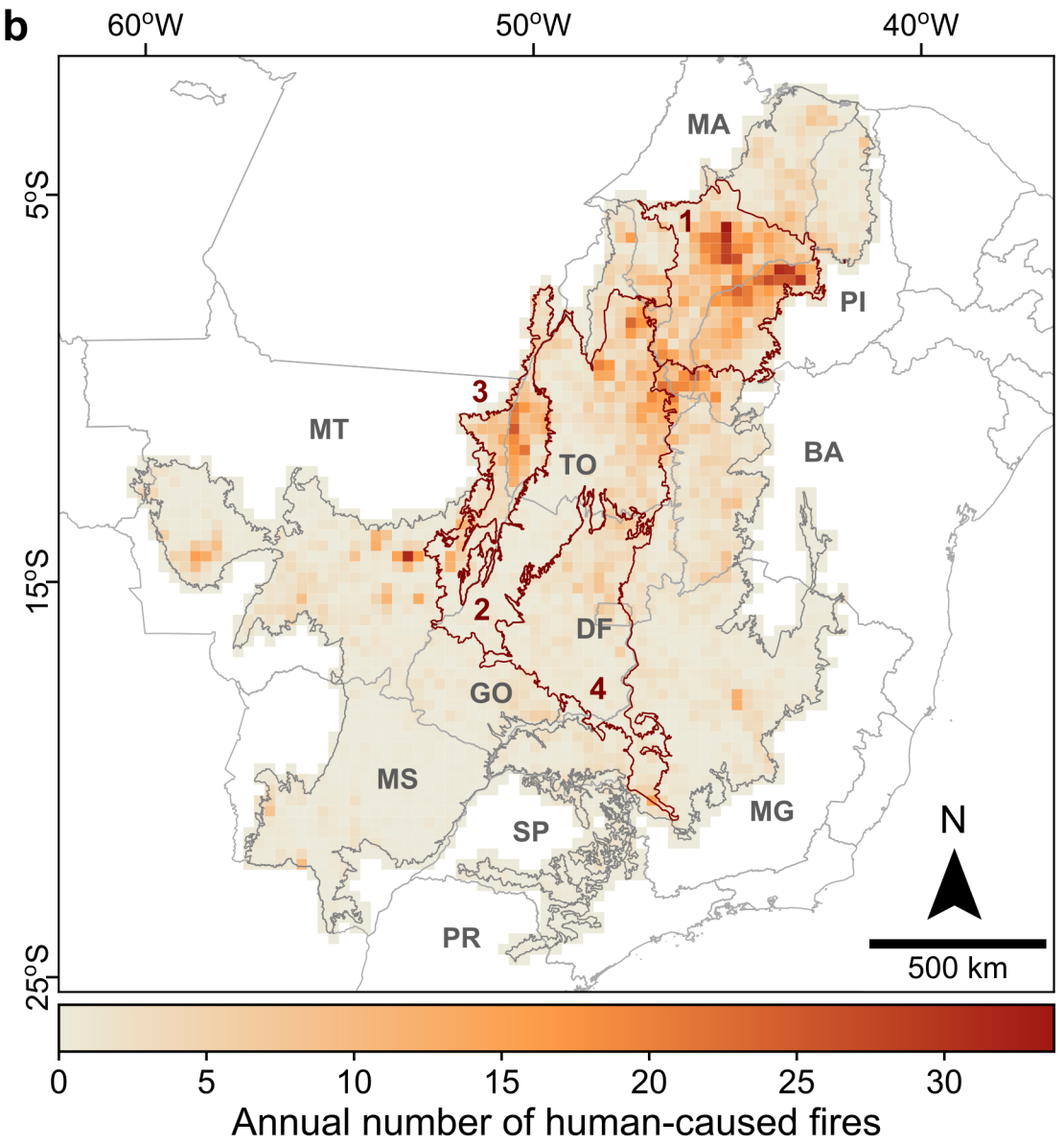
b
60°W
50°W
40°W
5°S
15°S
25°S
MA
PI
MT
BA
TO
DF
GO
MS
SP
MG
PR
1
2
3
4
N
500 km
0
5
10
15
20
25
30
Annual number of human-caused fires

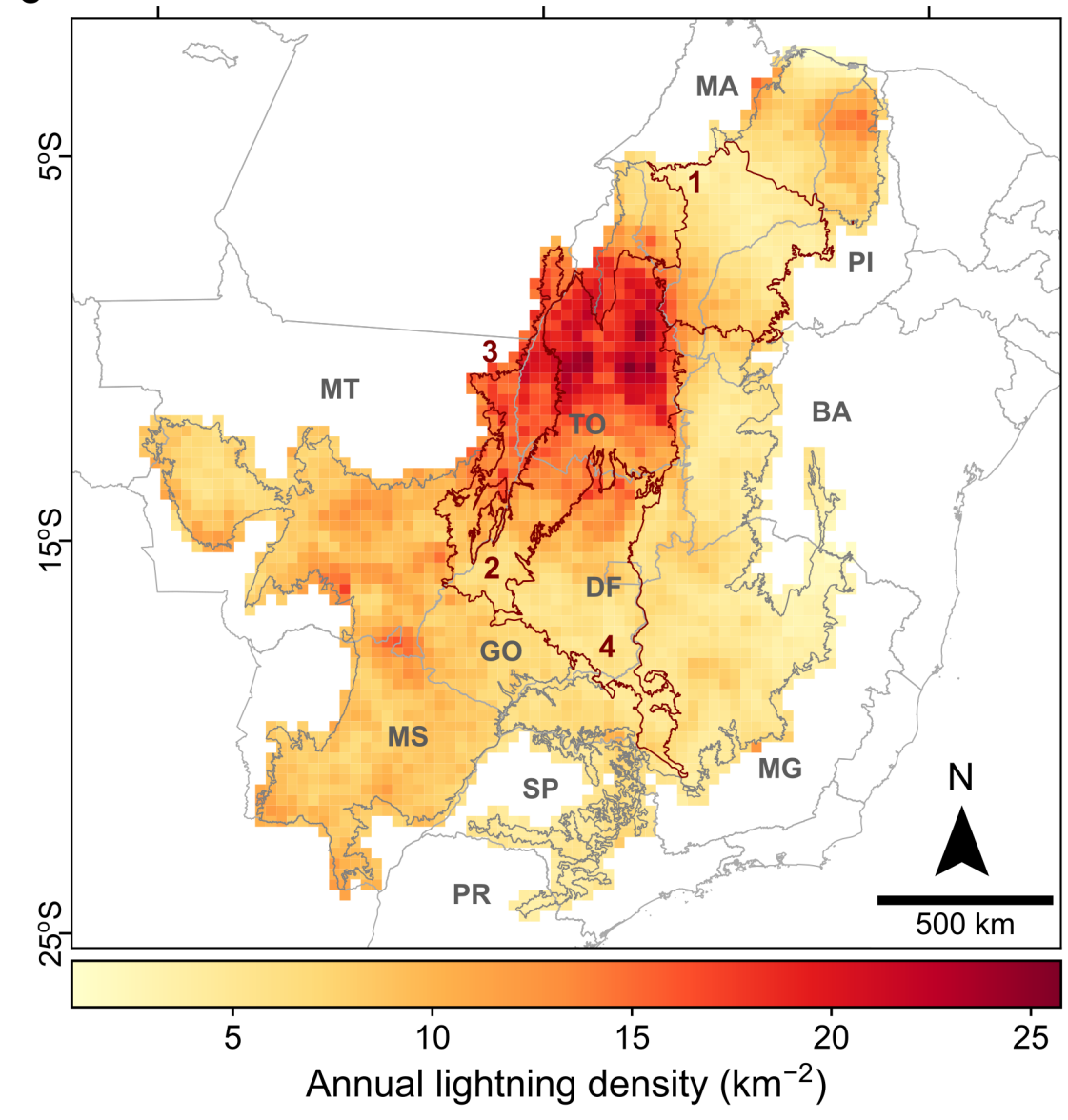
c
60°W
50°W
40°W
5°S
15°S
25°S
MA
PI
MT
BA
TO
DF
GO
MS
SP
MG
PR
1
2
3
4
N
500 km
5
10
15
20
25
Annual lightning density (km^{-2})

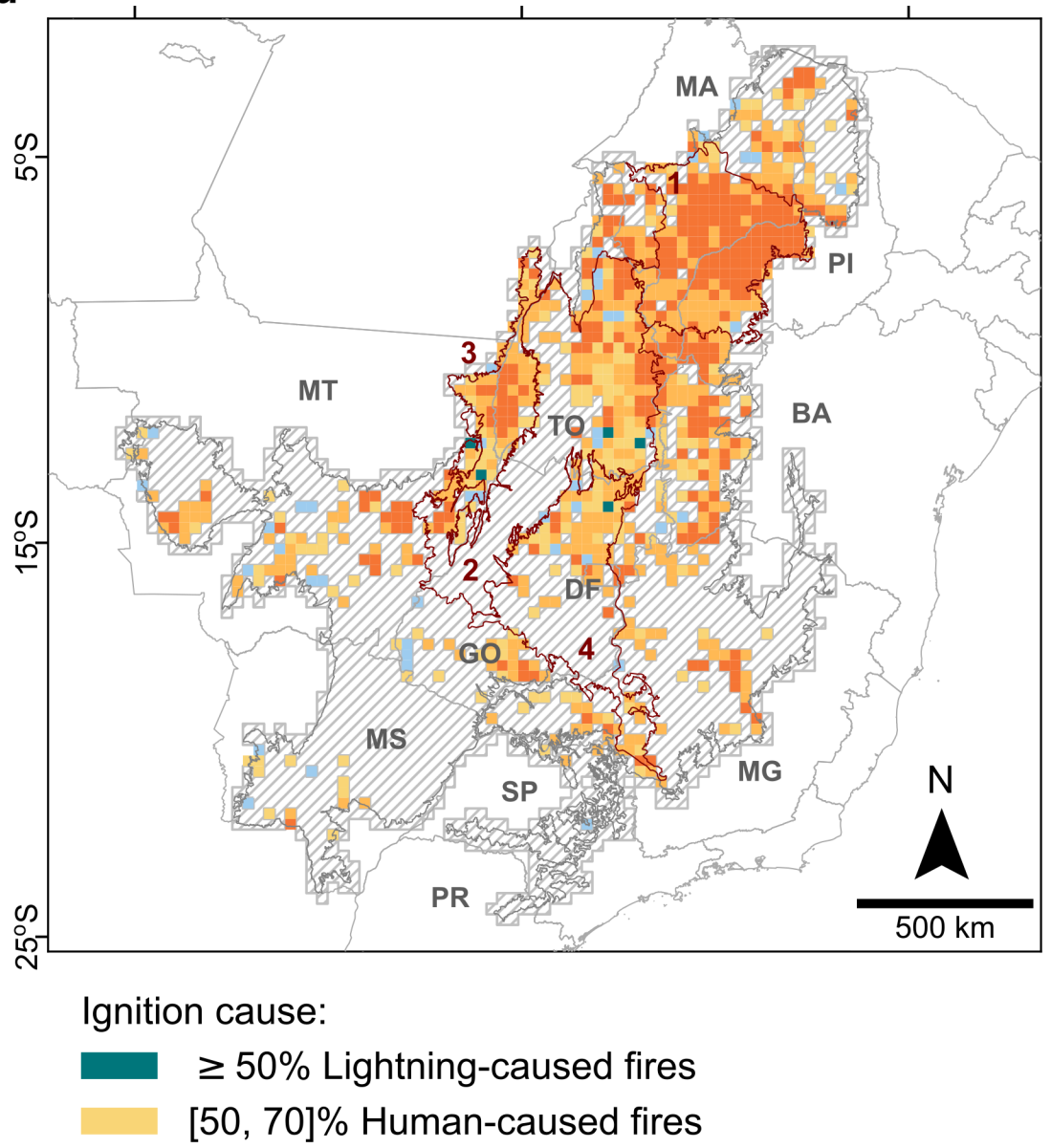
d
60°W
50°W
40°W
5°S
15°S
25°S
MA
PI
MT
BA
TO
DF
GO
MS
SP
MG
PR
1
2
3
4
N
500 km
Ignition cause:
≥ 50% Lightning-caused fires
[50, 70]% Human-caused fires
(70, 90]% Human-caused fires
> 90% Human-caused fires
No clear dominance
Not included in map (<10 fires)

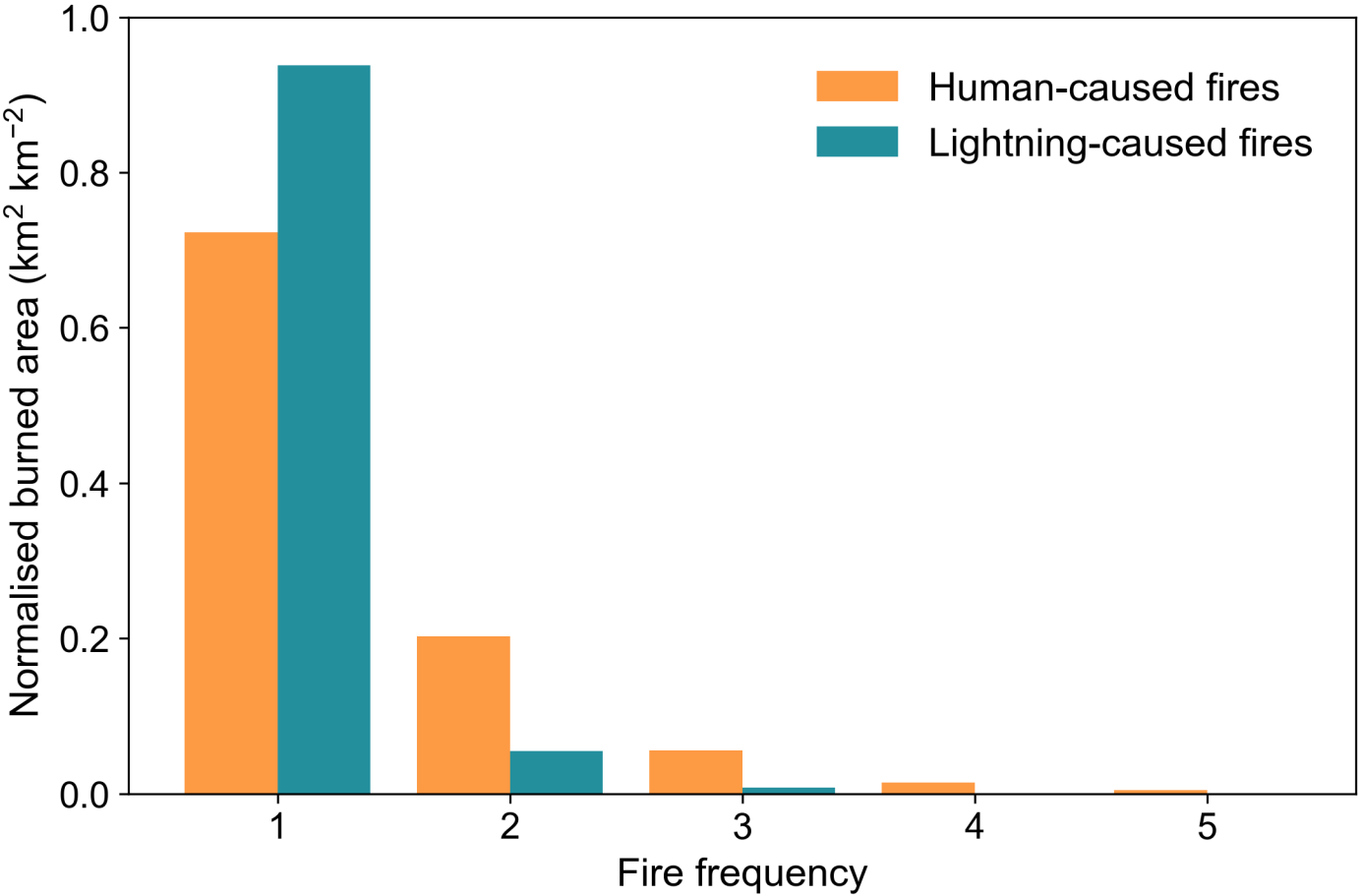
Human-caused fires
Lightning-caused fires
Normalised burned area (km^2 km^{-2})
1.0
0.8
0.6
0.4
0.2
0.0
1
2
3
4
5
Fire frequency

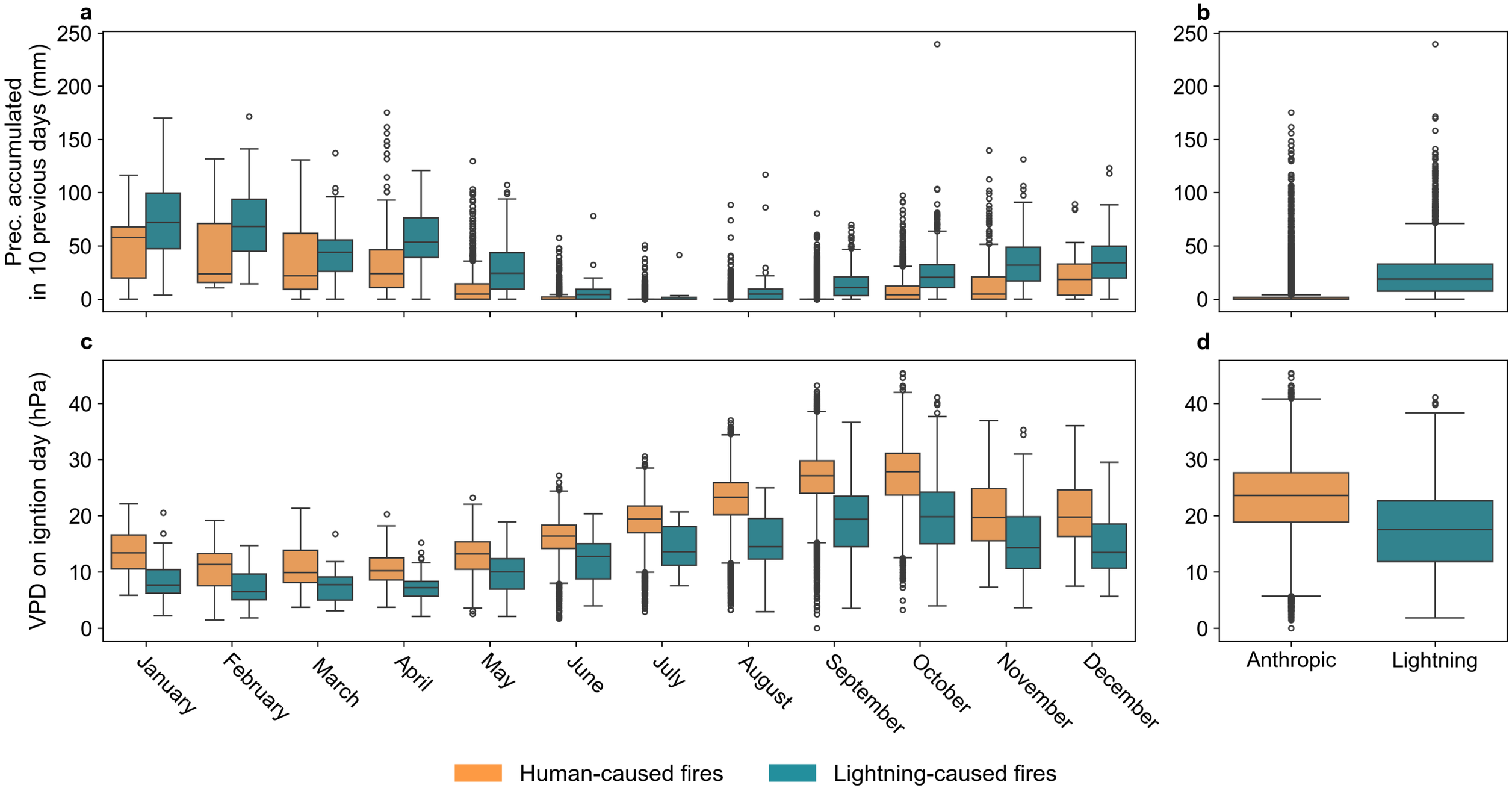
a
b
c
d
Prec. accumulated in 10 previous days (mm)
VPD on igntion day (hPa)
0
50
100
150
200
250
10
20
30
40
January
February
March
April
May
June
July
August
September
October
November
December
Anthropic
Lightning
Human-caused fires
Lightning-caused fires

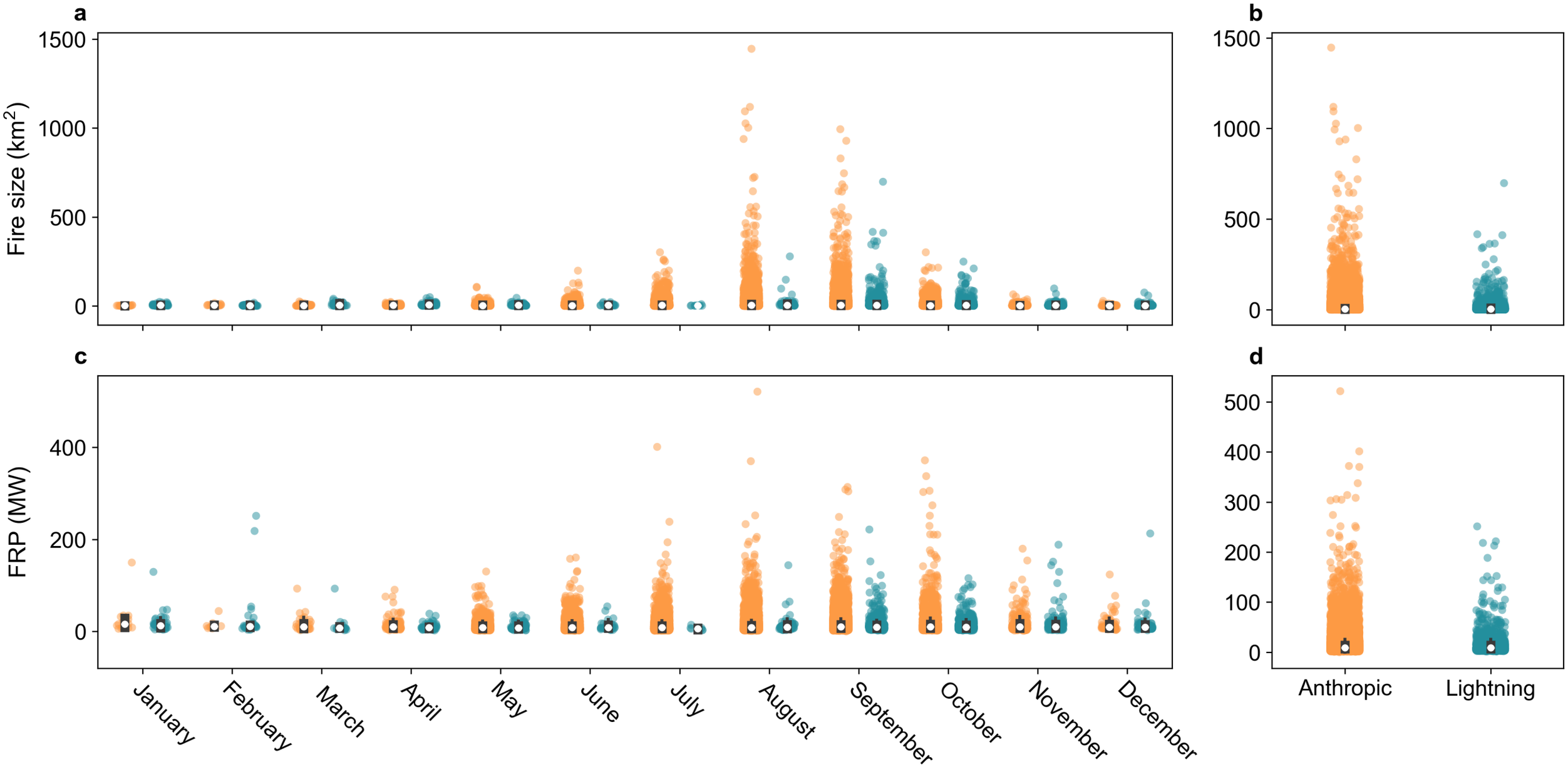
a
b
c
d
Fire size (km²)
FRP (MW)
1500
1000
500
0
400
200
300
100
January
February
March
April
May
June
July
August
September
October
November
December
Anthropic
Lightning
Human-caused fires
Lightning-caused fires

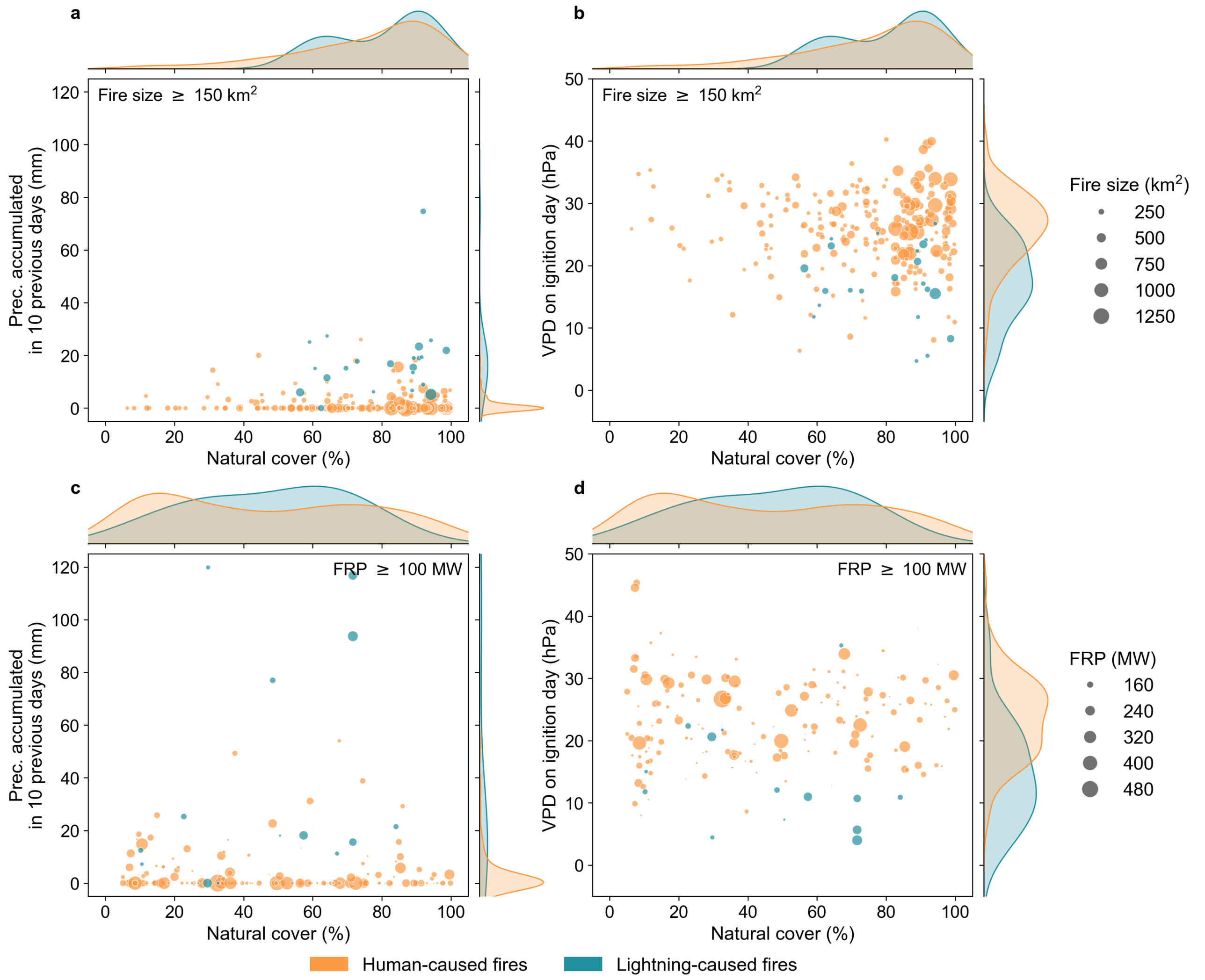
a
b
c
d
Fire size ≥ 150 km²
FRP ≥ 100 MW
Prec. accumulated in 10 previous days (mm)
VPD on ignition day (hPa)
Natural cover (%)
Fire size (km²)
250
500
750
1000
1250
FRP (MW)
160
240
320
400
480
Human-caused fires
Lightning-caused fires

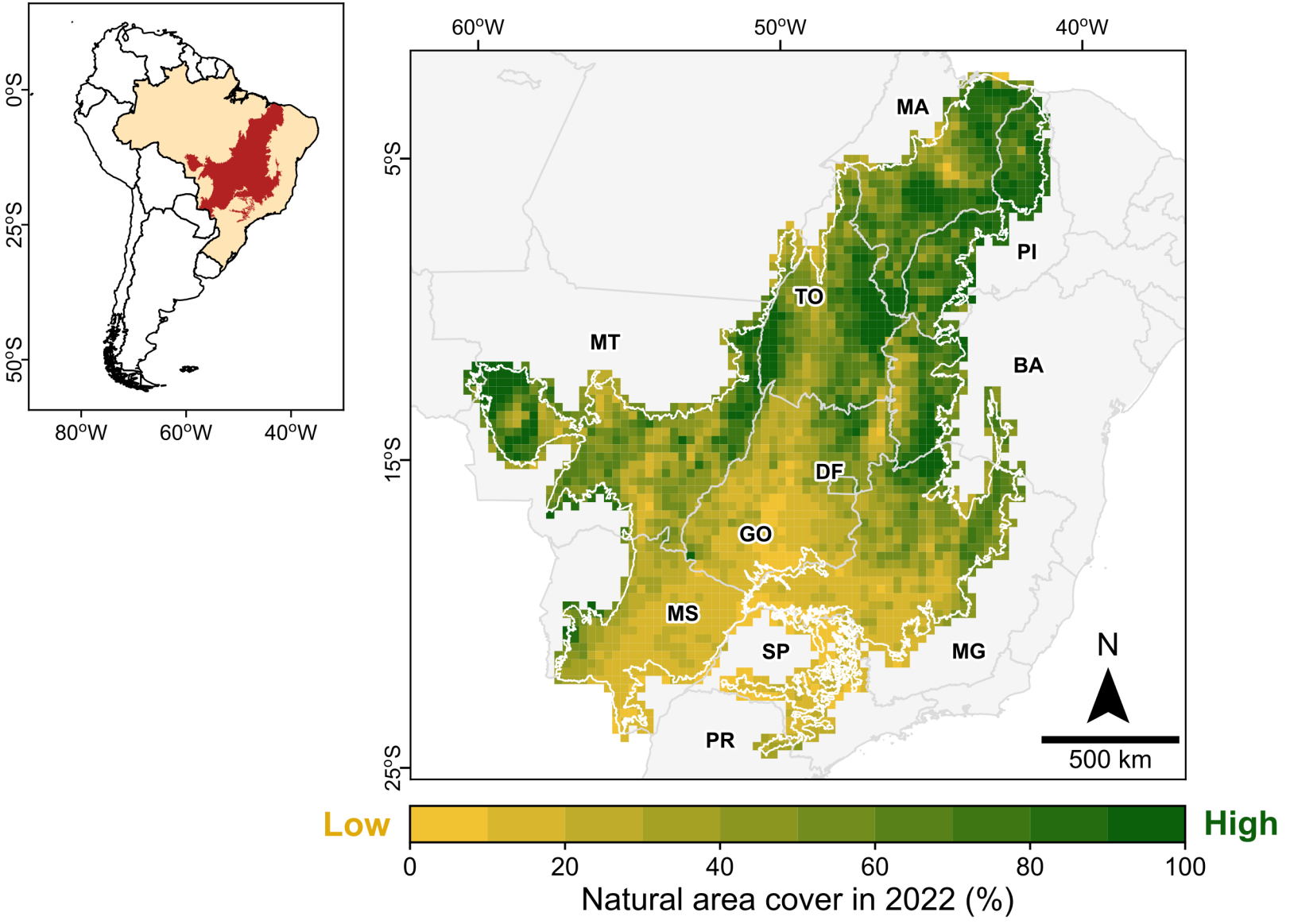
0°S
25°S
50°S
80°W
60°W
40°W
60°W
50°W
40°W
5°S
15°S
25°S
MA
PI
TO
MT
BA
DF
GO
MS
SP
MG
PR
N
500 km
Low
High
0
20
40
60
80
100
Natural area cover in 2022 (%)